Journal of Sound and Vibration (1998) **211**(5), 843–875

NEW APPROACHES FOR THE STUDY OF NON-LINEAR OSCILLATORS

R. N. IYENGAR

Central Building Research Institute, *Roorkee* 247667, *India*

AND

D. ROY

Engineering Mechanics Research Corp., 907, *Barton Centre*, 84, *M.G. Road*, *Bangalore* 560 001, *India*

(*Received* 17 *May*, 1996, *and in final form* 10 *November* 1997)

This paper presents a power series approach to accurately obtain the damped separatrices for a class of unforced non-linear oscillators. This in turn delineates the basins of attraction of two or more stable attractors in the phase space. The method is illustrated by its applications to the unforced Duffing – Holmes' and blacklash oscillators. Next, a novel semi-analytical integration scheme, called the phase space linearization method (PSL) is developed to obtain stable and unstable periodic solutions of forced as well as unforced non-linear oscillators and also the damped separatrices. The performance of the proposed method has been tested against periodic solutions of three oscillators, namely Ueda's, Duffing-Holmes' and Van der Pol's oscillators, obtained using a fourth order Runge-Kutta method with a sufficiently small time step. Moreover, the separatrices obtained using the PSL method are compared with those obtained via the power series method as developed earlier. The issue of accumulation of error in the PSL method as against the fourth order Runge-Kutta scheme is also described numerically through an example of a first order non-linear equation having closed form solution.

1. INTRODUCTION

Non-linear oscillators often possess more than one attractor in the phase space. Each of these attractors has its own basin of attraction, separated by curves or surfaces of measure zero, called separatrices. Determination of these separatrices allows one to demarcate the basins of attraction uniquely and therefore assumes importance in studying the global non-linear response of oscillators. A typical such oscillator is the cubic oscillator with negative linear stiffness, sometimes referred to as the Duffing-Holmes' oscillator. The phase plane diagrams for this oscillator without and with viscous damping and without external excitations are shown in Figures 1 and 2. A brute-force approach to find out the separatrices is to choose a sufficiently large set of initial conditions to cover the phase space of interest and then to integrate the ODE with each of these initial conditions to ascertain the attractor that the solution trajectory converges to. This approach is, however, computationally expensive and time consuming. Unfortunately existing theories of stability provide only sufficient conditions and therefore a computational approach for finding out the global domains of attraction needs to be iterative in general. Thus, Margolis and Vogt [1] have recursively used a method based on Liapunov functions originally proposed by Zubov [2] to determine the regions of attraction of second order systems. A

0022–460X/98/150843 + 33 $25.00/0/sv971429

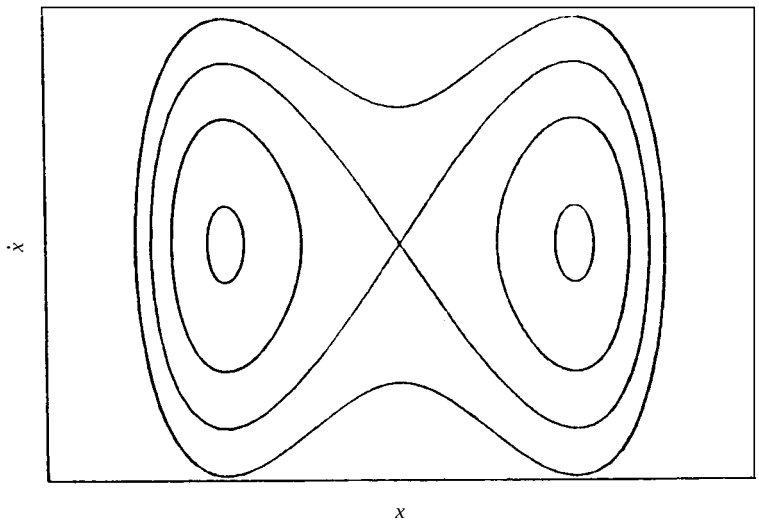

Figure 1. Phase plane diagram for the undamped and unforced Duffing-Holmes' oscillator.

drawback of this technique is the non-uniform convergence arising out of a Taylor-series expansion of the non-linear term. Davison and Kurak [3] have fitted a hyperellipse in the domain of attraction. The hyperellipse was determined using a constrained error minimization. However, this method is not designed to determine the complete domain of attraction. For autonomous non-linear systems, Vannellij and Vidyasagar [4] have exploited the concept of maximal Liapunov function to develop a partial differential equation (PDE) that provides the basis for obtaining the regions of attraction. However, the solution of this PDE itself is a formidable task. For many oscillators which show chaos, an analysis of the separatrices may provide a valuable guide towards understanding the onset of chaos. With this in mind, an effort is made in this paper to analytically obtain

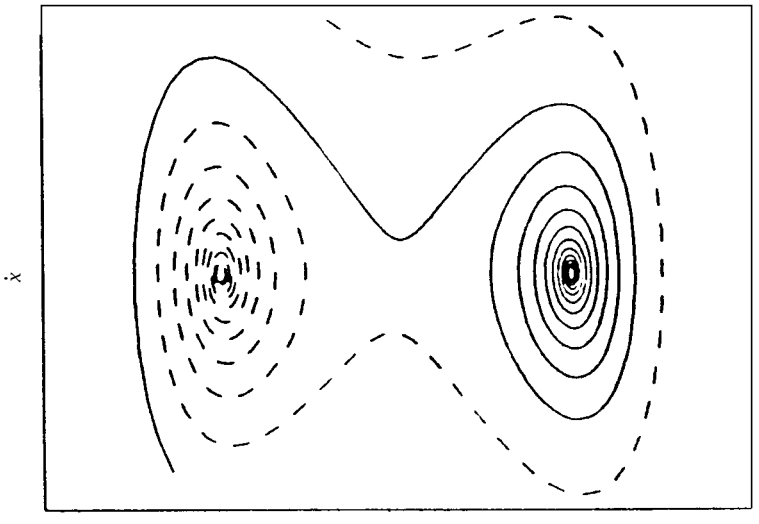

Figure 2. Asymptotic positions of a pair of trajectories starting from different initial conditions.

the separatrices of a class of second order non-linear oscillators having two-well potential based on a *power series approach*.

Even though the power series approach was found to be a powerful analytical tool to delineate the basins of attractions of the stable fixed points for the unforced oscillators, such an approach cannot readily be adapted to find out the separatrices when the oscillators are forced by harmonic excitations. In such a case, the unstable saddles, through which the separatrices pass, Hopf-bifurcate into unstable limit cycles. Thus, it is important to accurately find out the unstable limit cycle before an attempt can be made to obtain the forced separatrix. Unfortunately, existing numerical methods of integration, such as the Runge-Kutta method, the Milne method or the Adams–Bashforth method, cannot be used for finding the unstable orbits. Moreover, all these numerical schemes essentially convert the continuous flow of the original ODE to a finite difference map, which is iterated to proceed forward in time. In view of this, a new semi-analytical method for integrating non-linear ODEs is further developed in this paper. The method is based on successive linearization of the vector field in the phase space. The basic idea behind this new method is first introduced. Then the method is applied to obtain the periodic response of three distinct kinds of non-linear oscillators. The first one is Ueda's oscillator, which, when unperturbed, i.e., undamped and unforced, possesses no hyperbolic fixed points in the phase plane. This is in contrast to the Duffing-Holmes oscillator, which has a saddle along with a pair of centres in the unperturbed phase plane. The third example is the Van der Pol oscillator, which provides a prototypical example of self-excited non-linear oscillators. Comparisons of this new technique with the conventional Runge-Kutta method are also furnished. To have an estimate of the error getting accrued in the marching process, the solutions obtained via the new method and the Runge-Kutta method are compared with the known exact solution of a first order non-linear ODE. The method is then adapted to obtain the damped separatrices of a class of double well potential problems and compared with the power series solutions developed earlier. Finally the new method is exploited to find out a class of stable and unstable limit cycles with relatively less numerical effort.

2. THE NON-LINEAR OSCILLATORS

Four different non-linear oscillators are dealt with in the present paper. These are the cubic oscillators with (Duffing-Holmes') and without (Ueda's) the linear stiffness term, the backlash oscillator and the Van der Pol's oscillator. The Duffing-Holmes' oscillator is given by the following second order ODE

$$\ddot{z} + c\dot{z} - k_1 z + k_2 z^3 = P \cos(\lambda t). \tag{1}$$

Here dots denote differentiation with respect to time t. There are five parameters, namely c, k_1, k_2, P and λ, and all of them will be considered to be non-negative real numbers. It is convenient to reduce these five parameters to three via the following set of transformations

$$x = \frac{z}{z_c},$$

$$z_c = \left(\frac{k_1}{k_2}\right)^{1/2},$$

$$\tau = \frac{\lambda t}{2\pi}. \tag{2}$$

This results in

$$x'' + 2\pi\varepsilon_1 x' + 4\pi^2\varepsilon_2 (x^3 - x) = 4\pi^2\varepsilon_3 \cos(2\pi t), \tag{3}$$

where primes denote derivatives with respect to the normalized time, τ. However, for further discussion, primes will be replaced by dots and τ by t. In Ueda's equation the linear term is not present and hence can be expressed as

$$\ddot{x} + 2\pi\varepsilon_1 \dot{x} + 4\pi^2\varepsilon_2 x^3 = 4\pi^2\varepsilon_3 \cos(2\pi t). \tag{4}$$

In contrast with the above two oscillators, the backlash oscillator is piecewise linear and is given by the following second order ODE

$$\ddot{x} + \varepsilon_1 \dot{x} = 0 \quad |x| \leqslant h,$$

$$\ddot{x} + \varepsilon_1 \dot{x} + \varepsilon_2 (x - h \operatorname{sgn} x) = 0 \quad |x| \geq h, \tag{5}$$

where h is a positive real number. The normalized form of Van der Pol's oscillator is

$$\ddot{x} + 2\pi\varepsilon_1 \dot{x}(4x^2 - 1) + 4\pi^2\varepsilon_2 x = 4\pi^2\varepsilon_3 \cos(2\pi t). \tag{6}$$

3. DAMPED SEPARATRIX: POWER SERIES SOLUTION

Equation (3) for $\varepsilon_3 = 0$ possesses an unstable solution which approaches zero asymptotically. In the phase plane, this passes through the origin. This is called the damped separatrix. Now equation (3), with $\varepsilon_3 = 0$, is recast as

$$y = \dot{x},$$

$$\dot{y} = -\delta_1 y - \delta_2 (x^3 - x), \tag{7}$$

where

$$\delta_1 = 2\pi\varepsilon_1,$$

$$\delta_2 = 4\pi^2\varepsilon_2. \tag{8}$$

Elimination of the independent time variable from equation (7) results in

$$y \frac{dy}{dx} + \delta_1 y = -\delta_2 (x^3 - x). \tag{9}$$

Equation (9) has two sinks at $\{\pm 1, 0\}$ and a saddle at $\{0, 0\}$. It is intended, here, to closely approximate the separatrix, separating the basins of attraction of the two sinks, as shown in Figure 3. Now, in order to approximate the separatrix near the saddle $\{0, 0\}$, y is expanded in terms of a power series in x around the saddle as

$$y = a_0 + a_1 x + a_2 x^2 + a_3 x^3 + \cdots, \tag{10}$$

so that

$$\frac{dy}{dx} = \sum_{n=1}^{\infty} n a_n x^{n-1}. \tag{11}$$

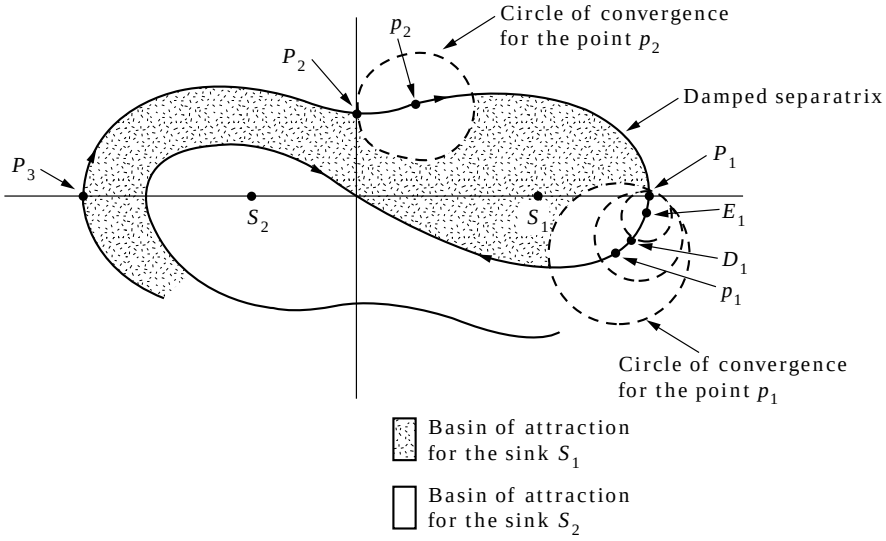

Figure 3. Damped separatrices and convergence of the power series.

The condition $y(x = 0)$ yields $a_0 = 0$. The other coefficients may be readily obtained by substituting equations (10) and (11) in equation (9) followed by equating the various powers of x. Thus

$$x^1: \quad a_1 = -0{\cdot}5\delta_1 \pm 0{\cdot}5(\delta_1^2 + 4\delta_2)^{1/2},$$

$$x^2: \quad a_2 = 0$$

$$x^3: \quad a_3 = \frac{-\delta_2}{(4a_1 + \delta_1)},$$

$$x^4: \quad a_4 = 0,$$

$$x^5: \quad a_5 = \frac{-3a_3^2}{(6a_1 + \delta_1)},$$

$$\text{and so on } \ldots . \tag{12}$$

The ambiguity associated with the coefficient a_1 may be resolved by noting that, very near the saddle, where $a_1 x$ is the major contributing term in equation (10), y is negative for positive x and vice versa. This leads to

$$a_1 = -0{\cdot}5\delta_1 - 0{\cdot}5(\delta_1^2 + 4\delta_2)^{1/2}. \tag{13}$$

Referring to Figure 3, it may be argued that the power series in equation (10) would converge at a point p near the saddle within a circle of radius R, where R is the distance of p from the nearest pole P_1. At P_1, $\mathrm{d}y/\mathrm{d}x$ becomes unbounded. Therefore, as the pole P_1 is approached, R decreases and obviously more and more terms in the power series expansion (10) would have to be retained for convergence. This can, however, be avoided if the pole P_1 is vaulted. To this end, some point $p_1 = \{x_1, y_1\}$ is chosen away from P_1. Now by introducing linear transformations

$$x = \bar{x} + x_1,$$

$$y = \bar{y} + y_1, \tag{14}$$

equation (9) takes the form

$$-\frac{\mathrm{d}\bar{x}}{\mathrm{d}\bar{y}}\{\delta_1(\bar{y}+y_1)+\delta_2(\bar{x}^3+3\bar{x}^2x_1+3\bar{x}x_1^2+x_1^3-\bar{x}-x_1)\}=y_1+\bar{y}. \tag{15}$$

It is noted that the separatrix is unique and the function relating y and x (or $\bar{y}$ and $\bar{x}$) over a small segment is one-to-one and hence invertible. Thus, it is possible to expand $\bar{x}$ as a power series in $\bar{y}$ around the point p_1 as follows

$$\bar{x}=\sum_{i=0}^{\infty} b_i\,\bar{y}^i. \tag{16}$$

It immediately follows that $b_0=0$. The other coefficients may be evaluated by substituting equation (16) into equation (15) and equating various powers of $\bar{y}$. They are

$$\begin{aligned}
\bar{y}^0\text{:}\quad & b_1=\frac{y_0}{\{\delta_1 y_1+\delta_2(x_1^3-x_1)\}},\\
\bar{y}^1\text{:}\quad & b_2=0{\cdot}5\{1+\delta_1 b_1+b_1^2\delta_2(3x_1^2-1)\}/(\delta_2 x_1-\delta_2 x_1^3-\delta_1 y_1),\\
& \cdots\cdots\cdots
\end{aligned} \tag{17}$$

The power series in equation (16) would fail to converge at the pole P_2. Therefore, again a point $p_2=\{x_2, y_2\}$ away from P_2 is chosen and the following transformation introduced

$$\begin{aligned}
x&=\bar{x}+x_2,\\
y&=\bar{y}+y_2.
\end{aligned} \tag{18}$$

The variable $\bar{y}$ is now expanded in a power series in $\bar{x}$ around p_2 as

$$\bar{y}=\sum_{i=0}^{\infty}\mathrm{d}_i\,\bar{x}^i. \tag{19}$$

Using equation (18) in equation (9), it follows that

$$\frac{\mathrm{d}\bar{y}}{\mathrm{d}\bar{x}}\bar{y}+y_2\frac{\mathrm{d}\bar{y}}{\mathrm{d}\bar{x}}+\delta_1\bar{y}=-\delta_2(\bar{x}^3+3\bar{x}^2x_2+3\bar{x}x_2^2+x_2^3-\bar{x}-x_2)-\delta_1 y_2. \tag{20}$$

The coefficients d_i may now be evaluated on similar lines as explained earlier. This technique of switching to and fro in between the power series in equation (16) and the one in equation (19) may be continued to avoid the consecutive poles and in the process, as many loops of the damped separatrix may be generated as desired.

It may be pointed out here that the analysis of the damped separatrices as presented above applies to many other damped non-linear oscillators, where such separatrices exist. This is true even for a class of oscillators where the vector field is not always C^r, $r>1$. As an interesting example, the piecewise linear viscously damped backlash oscillator as described by equation (5) may be taken up. It may be readily observed that every point in $[-h, h]$ is a non-hyperbolic (or neutrally stable) sink of the oscillator. The oscillator therefore has an uncountable infinity of such neutrally stable sinks. As $t\to\infty$ every trajectory of the oscillator almost surely approaches a point either in the left half $[-h, 0)$ or in the right half $(0, h]$ with a damped separatrix passing through $\{0, 0\}$. However, it is worth mentioning here that this separatrix is not a homoclinic orbit since the point $\{0, 0\}$ is not a saddle. The two eigenvalues determining the nature of solution trajectories at and near $\{0, 0\}$ are $-h$ and 0. The negative eigenvalue, $-h$, determines the exponential rate with which a point chosen on the separatrix away from $\{0, 0\}$ gets attracted to nor repelled by the separatrix. Thus, such an orbit asymptotically reaches a point either on the left half,

$[-h, 0)$, or on the right half, $(0, h]$, of the x-axis. Here the oribt passing exactly through $\{0, 0\}$ is called the separatrix, as it enables one to identify whether an arbitrarily chosen initial condition ends up on the left or right of $\{0, 0\}$.

In order to find out this separatrix, the power series approach can again be used. The method is very much similar to the one described for the Duffing-Holmes' oscillator. First, the equation (5) is cast in the form

$$\frac{dy}{dx} = +\varepsilon_1 \qquad \text{if } |x| < h,$$

$$\frac{dy}{dx} = \frac{-\varepsilon_1 y - \varepsilon_2 (x - h)}{y} \qquad \text{if } |x| \geq h, \tag{21}$$

where $y = \dot{x}$. As has been seen for Duffing–Holmes' oscillator, the power series approach needs to be applied over small segments of the orbit so that successive poles are suitably vaulted. With this in view, it is advantageous to introduce the following transformations

$$x = \bar{x} + x_i,$$

$$y = \bar{y} + y_i, \tag{22}$$

where $\{x_i, y_i\}$ denote the co-ordinates of the last known point on the separatrix. For example, to start with $\{x_0, y_0\}$ will be the same as the origin $\{0, 0\}$. Thus, one has

$$\frac{d\bar{y}}{d\bar{x}} = -\varepsilon_1 \qquad \text{if } |x| < h,$$

$$\frac{d\bar{y}}{d\bar{x}}\bar{y} + \frac{d\bar{y}'}{d\bar{x}} y_i + \varepsilon_1 \bar{y} = -\varepsilon_2 (\bar{x} + x_i - h) - \varepsilon_1 y_i \qquad \text{if } |x| \geq h,$$

$$= -\varepsilon_2 (\bar{x} + x_i + h) - \varepsilon_1 y_i \qquad \text{if } |x| \geq h. \tag{23}$$

Now $\bar{y}$ is expanded as a power series in $\bar{x}$ as

$$\bar{y} = \sum_{i=1}^{\infty} a_i \bar{x}^i. \tag{24}$$

The coefficients a_i are

$$\bar{x}^0: \quad a_1 = \frac{-\varepsilon_1 y_i + \varepsilon_2 (x_i - h \operatorname{sgn} x_i)}{y_i},$$

$$\bar{x}^1: \quad a_2 = -\frac{\varepsilon_2 + \varepsilon_1 a_1 + a_1^2}{2y_i},$$

$$\bar{x}^2: \quad a_3 = -\frac{a_2 (\varepsilon_1 + 3a_1)}{3y_i},$$

$$\bar{x}^3: \quad a_4 = -\frac{\varepsilon_1 a_3 + 2a_2^2 + 4a_1 a_3}{4y_i},$$

$$\bar{x}^4: \quad a_5 = -\frac{\varepsilon_1 a_4 + 5a_2 a_3 + 5a_1 a_4}{5y_i},$$

$$\ldots\ldots\ldots \tag{25}$$

As a pole is approached $\mathrm{d}\bar{y}/\mathrm{d}\bar{x}$ becomes unbounded. In order to vault the pole, $\bar{x}$ is expanded as a power series in $\bar{y}$ as in equation (16). Next, the coefficients b_i are given by

$$\begin{aligned}
\bar{y}^0: \quad & b_1 = -\frac{y_i}{\varepsilon_1 y_i + \varepsilon_2 (x_i - h \operatorname{sgn} x_i)}, \\
\bar{y}^1: \quad & b_2 = -\frac{1 + \varepsilon_1 b_1 + \varepsilon_2 b_1^2}{2\varepsilon_1 y_i + 2\varepsilon_2 (x_i - h \operatorname{sgn} x_i)}, \\
\bar{y}^2: \quad & b_3 = -\frac{2b_2 \varepsilon_1 + 3b_1 b_2 \varepsilon_2}{3\varepsilon_1 y_i + 3\varepsilon_2 (x_i - h \operatorname{sgn} x_i)}, \\
\bar{y}^3: \quad & b_4 = -\frac{-3\varepsilon_1 b_3 + 2\varepsilon_2 (2b_1 b_3 + b_2^2)}{4\varepsilon_1 y_i + 4\varepsilon_2 (x_i - h \operatorname{sgn} x_i)}, \\
\bar{y}^4: \quad & b_5 = -\frac{4\varepsilon_1 b_4 + 5\varepsilon_2 (b_1 b_4 + b_2 b_3)}{5\varepsilon_1 y_i + 5\varepsilon_2 (x_i - h \operatorname{sgn} x_i)}, \\
& \ldots\ldots\ldots
\end{aligned} \tag{26}$$

3.1. NUMERICAL RESULTS

To illustrate the foregoing analysis, some numerical results have been obtained. First, the damped Duffing-Holmes' oscillator is taken up. Figure 4(a–c) shows the damped separatrices obtained using the power series approach for different values of the damping parameter, ε_1. The method has been found to be extremely efficient from a computational viewpoint. Here, to reduce the number of terms in the power series given by the equations (16) and (19), the following numerical strategy has been resorted to. Power series (16) has been used as long as $|\mathrm{d}\bar{x}/\mathrm{d}\bar{y}| \leq 1$. If $|\mathrm{d}\bar{x}/\mathrm{d}\bar{y}| > 1$, it implies that $|\mathrm{d}\bar{y}/\mathrm{d}\bar{x}| < 1$, and in such a situation power series (19) has been made use of. Again for $|\mathrm{d}\bar{y}/\mathrm{d}\bar{x}| > 1$, a switch-over to the power series in equation (16) has been effected. For the backlash oscillator given by equation (5), the damped separatrices have been obtained for three different values of the damping parameter, ε_1, and these are shown in Figure 5. The discontinuities of these separatrices at $|x| = h$ are quite conspicuous.

4. THE CONCEPT OF LINEARIZATION

It is quite well known that for obtaining the one-periodic response of a non-linear oscillator driven by a harmonic excitation, it is possible to replace the non-linear system by an equivalent linear system with the same excitation. The technique is known as the linearization of Krylov and Bogliubov and has been well documented by Minorsky [6]. In this method the mean square error due to the replacement of the non-linear flow by a linear flow is minimized with respect to the unknown parameters over one cycle of oscillation. Since the steady-state response of the equivalent linear system has to be in the form of a symmetric one-periodic orbit around a fixed point, one ends up with an approximation to the actual orbit under certain restrictions.

The concept of local linearizations of non-linear vector fields around fixed points, or more generally non-wandering sets, is also well studied in the literature on non-linear dynamical systems. In particular, it is known from Hartman's theorem that if p is a hyperbolic fixed point of the non-linear oscillator, then there is a C^0 invertible map (homeomorphism) locally taking the actual orbit to the orbit of the linearized variational equation, defined by

$$\dot{y} = D_x (p) y, \tag{27}$$

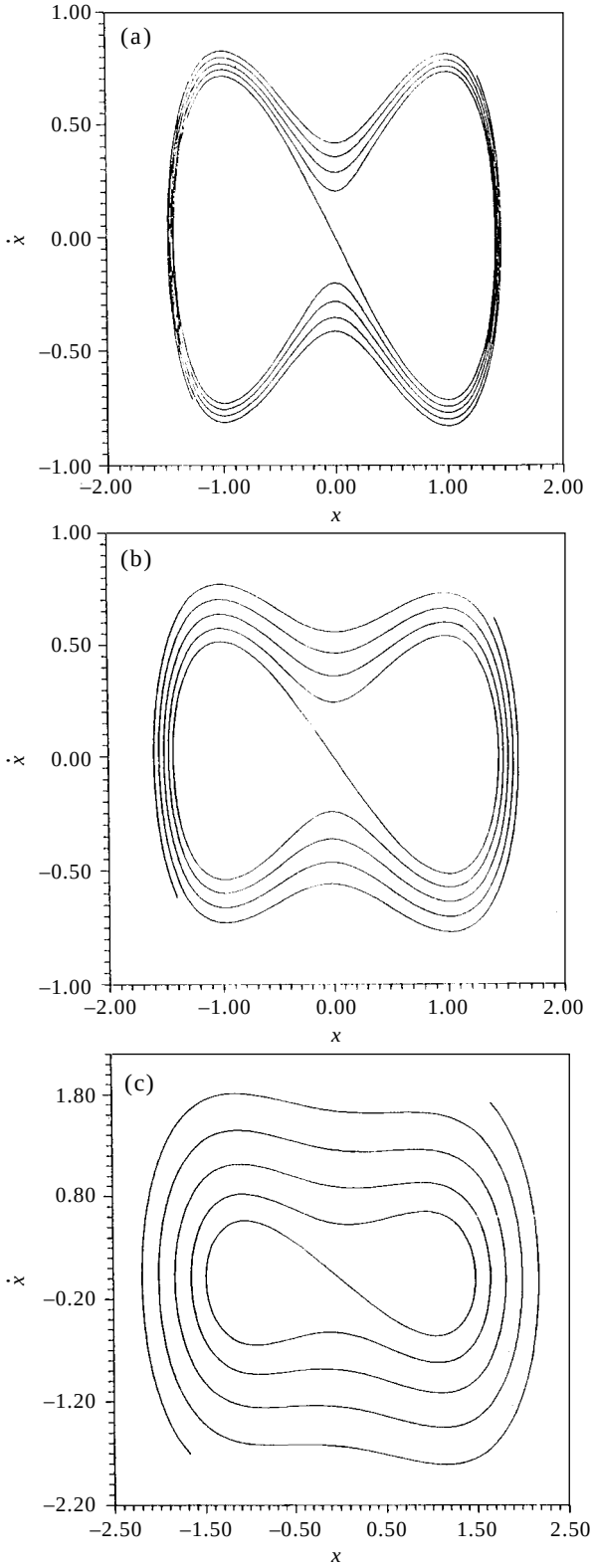

Figure 4. Damped separatrices for Duffing-Holmes' oscillator via power series: (a) $\varepsilon_1 = 0{\cdot}01$, $\varepsilon_2 = 0{\cdot}5$, $\varepsilon_3 = 0$; (b) $\varepsilon_1 = 0{\cdot}1$, $\varepsilon_2 = 0{\cdot}5$, $\varepsilon_3 = 0$; (c) $\varepsilon_1 = 0{\cdot}25$, $\varepsilon_2 = 0{\cdot}5$, $\varepsilon_3 = 0$.

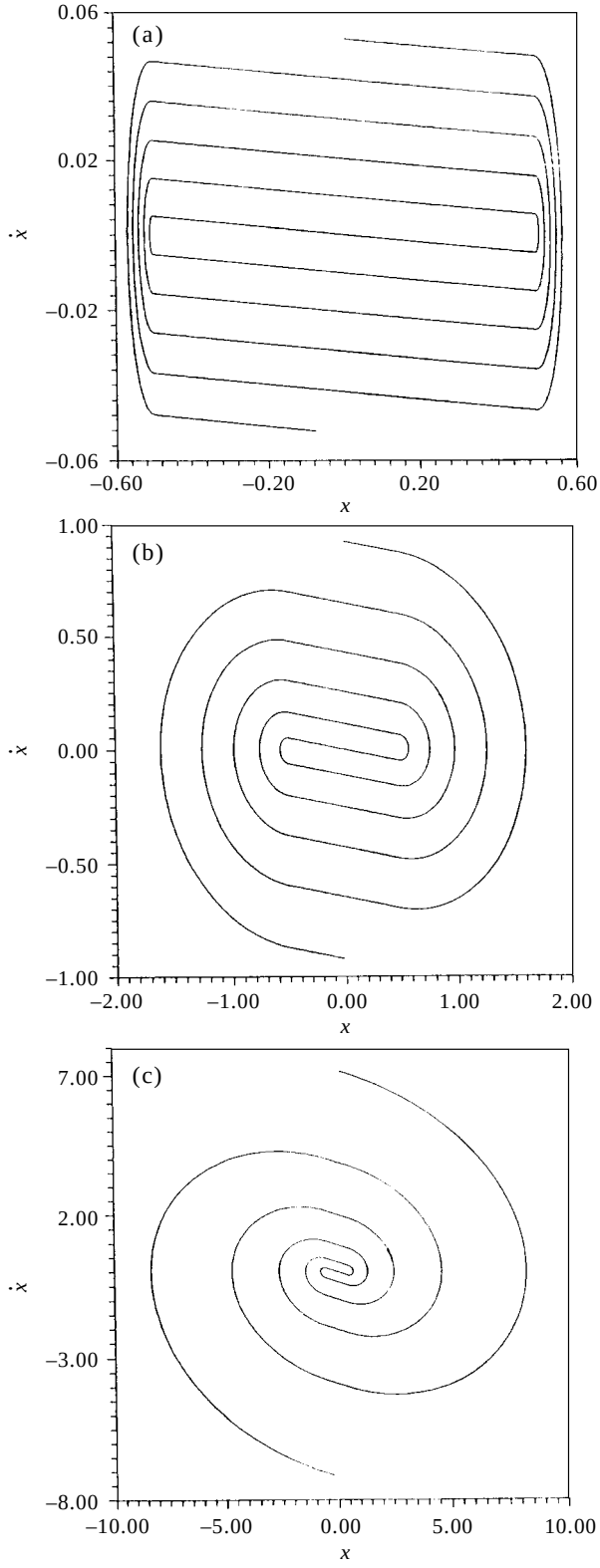

Figure 5. Damped separatrices for the backlash oscillator via power series: (a) $\varepsilon_1 = 0{\cdot}05$, $\varepsilon_2 = 0{\cdot}5$, $h = 0{\cdot}5$; (b) $\varepsilon_1 = 0{\cdot}15$, $\varepsilon_2 = 0{\cdot}5$, $h = 0{\cdot}5$; (c) $\varepsilon_1 = 0{\cdot}5$, $\varepsilon_2 = 0{\cdot}5$, $h = 0{\cdot}5$.

where x is the original co-ordinate vector. However, there is no way to explicitly construct this homeomorphism and, moreover, away from the fixed point, p, Hartman's theorem is no longer valid.

5. PHASE SPACE LINEARIZATION (PSL)

To start with, the non-linear ODE

$$\ddot{x} + c\dot{x} + kx + \xi(x, \dot{x}) = F \sin(\lambda t), \qquad x \in \mathbf{R}^1, \tag{28}$$

with the initial conditions

$$x(t_0) = x_0,$$

$$\dot{x}(t_0) = \dot{x}_0,$$

is considered. Here the function ξ is non-linear in x and $\dot{x}$. Now, using the existence and uniqueness theorem [8], if the vector field is C^r, $r \geq 1$, and $\{x_0, \dot{x}_0, t_0\} \in U \subset \mathbf{R}^2 \times \mathbf{R}^1$, then there is a unique C^r local solution $\phi_t(x_0, \dot{x}_0, t)$ for $|t - t_0|$ sufficiently small. Moreover, the solution $\phi_t(x_0, \dot{x}_0, t)$ can be uniquely extended forward and backward in time provided it is bounded. At this stage, it is convenient to partially order the time axis as $t_0 < t_1 < t_2 < \cdots < t_i < t_{i+1} < \ldots$. Let the corresponding points on a solution trajectory be denoted as $\mathbf{x}_i = \{x_i, \dot{x}_i\}$, $i = 0, 1, 2, \ldots$ A knowledge of each of the solution segements $[\mathbf{x}_i, \mathbf{x}_{i+1}) \in \mathbf{R}^2$ allows one to construct the complete solution trajectory starting at $\mathbf{x}_0$ by taking the union $\cup_i [\mathbf{x}_i, \mathbf{x}_{i+1})$. Now, over the semi-closed time interval $[t_i, t_{i+1})$, the C^r solution trajectory $\mathbf{x}(\mathbf{x}_i, t_i, t)$ allows a Fourier series representation and thus it may be argued that over the same time interval it is possible to replace the non-linear ODE by an equivalent linear ODE, since the same Fourier representation is obtainable via a linear system. However, deriving such linear systems over each time interval is not an easy task. Presently, it would be interesting to ask whether it is possible to replace the non-linear term $\xi(x, \dot{x})$ by a suitably chosen linear function, leaving the other terms including the forcing unaffected. This would enable one to locally integrate the linear ODE to have a local approximation to the solution of the non-linear ODE over $[t_i, t_{i+1})$. The complete solution may then be obtained by simply joining the local solutions together. In what follows, an approximate replacement technique for the function $\xi(x, \dot{x})$ based on the minimization of errors is proposed. Thus, in the semi-closed interval $[t_i, t_{i+1})$ equation (28) may be replaced by the following linear ODE

$$\ddot{x} + c\dot{x} + kx + k_i(x_i, \dot{x}_i)x + c_i(x_i, \dot{x}_i)\dot{x} = F \sin(\lambda t). \tag{29}$$

Now to obtain workable expressions for k_i and c_i for every i, the square of the error

$$e_i^2 = \int_{x_i}^{x_i + \Delta_i} \int_{\dot{x}_i}^{\dot{x}_i + \gamma_i} \{\xi(x, \dot{x}) - k_i(x, \dot{x})x - c_i(x, \dot{x})\dot{x}\}^2 \, \mathrm{d}x \, \mathrm{d}\dot{x}, \tag{30}$$

may be minimized with respect to the unknown parameters, k_i and c_i. In the above expression, the increments Δ_i and γ_i are given by

$$\Delta_i = x_{i+1} - x_i,$$

$$\gamma_i = \dot{x}_{i+1} - \dot{x}_i. \tag{31}$$

This exercise finally results in a pair of non-linear algebraic equations in Δ_i and γ_i for each i. In the special cases where the function ξ in equation (28) is either of the following four forms

$$\xi = \xi(x),$$
$$\xi = \xi(\dot{x}),$$
$$\xi = \xi_1(\dot{x})x,$$
$$\xi = \xi_2(x)\dot{x}, \tag{32}$$

only a single transcendental equation for Δ_i or γ_i needs to be solved for each i.

To illustrate the implementation of the above linearization scheme, three examples, namely Ueda's oscillator, Duffing-Holmes' oscillator and Van der Pol's oscillator are taken up. Now to facilitate further discussion, it is convenient to recast equation (29) in the form

$$\ddot{x} + \eta(x_i, \dot{x}_i)\dot{x} + \beta(x_i, \dot{x}_i)x = F \sin(\lambda t). \tag{33}$$

5.1. UEDA'S OSCILLATOR

After a normalization, Ueda's oscillator is given by the non-linear ODE as in equation (4). Comparing the above equation with equation (28), it may be observed that

$$c = 2\pi\varepsilon_1,$$
$$k = 0,$$
$$\xi = 4\pi^2\varepsilon_2 x^3. \tag{34}$$

Here the equivalent linear equation (33) approximately valid over an interval $[t_i, t_{i+1})$ takes the form

$$\ddot{x} + 2\pi\varepsilon_1 \dot{x} + 4\pi^2\varepsilon_2 \beta(x_i)x = 4\pi^2\varepsilon_3 \cos(2\pi t). \tag{35}$$

Following an error minimization, i.e., $\partial e^2/\partial\beta = 0$, the expression for $\beta(x_i)$ is found to be

$$\beta(x_i) = (x_i^4 + 2x_i^3 \Delta_i + 2x_i^2 \Delta_i^2 + x_i \Delta_i^3 + \Delta_i^4/5)/(x_i^2 + x_i \Delta_i + \Delta_i^2/3), \tag{36}$$

where Δ_i is given by equation (31). The pair of eigenvalues associated with the complementary function of equation (35) are

$${}^i\lambda_{1,2} = -\pi\varepsilon_1 \pm \pi\sqrt{\{\varepsilon_1^2 - 4\varepsilon_2 \beta(x_i)\}}. \tag{37}$$

Now the particular solution of equation (35) is

$$p_i(t) = \frac{\varepsilon_3\{\varepsilon_2 \beta(x_i) - 1\}\cos(2\pi t) + \varepsilon_1 \varepsilon_3 \sin(2\pi t)}{\{\varepsilon_2 \beta(x_i) - 1\}^2 + \varepsilon_1^2}. \tag{38}$$

Letting

$$h_i = t_{i+1} - t_i, \tag{39}$$

the complete solution of equation (35) may, in general, be written down as

$$x(t) = F_{1i}(x_i, \dot{x}, \Delta_i, h_i),$$
$$\dot{x}(t) = \mathrm{d}F_{1i}/\mathrm{d}t = F_{2i}(x_i, \dot{x}_i, \Delta_i, h_i), \tag{40}$$

where

$$F_{1i} = K_{1i} \exp\{{}^i\lambda_1 (t - t_i)\} + K_{2i} \exp\{{}^i\lambda_2 (t - t_i)\} + p_i (t),$$
$$F_{2i} = {}^i\lambda_1 K_{1i} \exp\{{}^i\lambda_1 (t - t_i)\} + {}^i\lambda_2 K_{2i} \exp\{{}^i\lambda_2 (t - t_i)\} + \dot{p}_i (t),$$
$$\text{if } {}^i\lambda_{1,2} \text{ are real,} \tag{41}$$

otherwise

$$F_{1i} = \exp\{-\pi\varepsilon_1 (t - t_i)\} \{K_{1i} \cos(\pi\alpha_i t) + K_{2i} \sin(\pi\alpha_i t)\} + p_i (t),$$
$$F_{2i} = -\pi\varepsilon_1 \exp\{-\pi\varepsilon_1 (t - t_i)\} \{K_{1i} \cos(\pi\alpha_i t) + K_{2i} \sin(\pi\alpha_i t)\}$$
$$+ \pi\alpha_i \exp\{-\pi\varepsilon_1 (t - t_i)\} \{K_{2i} \cos(\pi\alpha_i t) - K_{1i} \sin(\pi\alpha_i t)\} + \dot{p}_i (t),$$
$$\alpha_i = \{4\varepsilon_2 \beta(x_i) - \varepsilon_1^2\}^{1/2}. \tag{42}$$

The constants K_{1i} and K_{2i} need to be determined from a knowledge of $\{x_i, \dot{x}_i\}$ followed by solving a pair of simultaneous equations. Now, Δ_i can be obtained using the identity

$$x_{i+1} = x_i + \Delta_i, \tag{43}$$

which leads to

$$\Delta_i = F_{1i} (x_i, \dot{x}_i, \Delta_i, t_{i+1}, h_i) - x_i. \tag{44}$$

The above is a transcendental equation in Δ_i and can be solved using standard routines. The original non-linear flow is thus converted to a 2-D non-linear map

$$x_{i+1} = F_{1i} (x_i, \dot{x}_i, \Delta_i, t_{i+1}, h_i),$$
$$x_{i+1} = F_{2i} (x_i, \dot{x}_i, \Delta_i, t_{i+1}, h_i). \tag{45}$$

This map may be iterated using a digital computer for as long as desired, provided the initial conditions x_0 and $\dot{x}_0$ along with the initial time, t_0, are prescribed.

5.2. DUFFING-HOLMES' OSCILLATOR

The normalized Duffing-Holmes' oscillator is given by equation (3). Comparison of this equation with equation (28) leads to

$$c = 2\pi\varepsilon_1,$$
$$k = -4\pi^2\varepsilon_2,$$
$$\xi = 4\pi^2\varepsilon_2 x^3. \tag{46}$$

The rest of the operations are very much similar to those carried out already for Ueda's oscillator. Thus, the equivalent linear equation along with its equivalent stiffness parameter $\beta(x_i)$ are again given by equations (35) and (36), respectively. The pair of eigenvalues ${}^i\lambda_{1,2}$ are now given by

$${}^i\lambda_{1,2} = -\pi\varepsilon_1 \pm \pi[\varepsilon_1^2 - 4\varepsilon_2 \{\beta(x_i) - 1\}]^{1/2}. \tag{47}$$

The particular solution is

$$p_i (t) = \frac{\varepsilon_3 [\varepsilon_2 \{\beta(x_i) - 1\} - 1] \cos(2\pi t)}{\{\varepsilon_2 (\beta(x_i) - 1) - 1\}^2 + \varepsilon_1^2}.$$
$$+ \frac{\varepsilon_1 \varepsilon_3 \sin(2\pi t)}{\{\varepsilon_2 (\beta(x_i) - 1) - 1\}^2 + \varepsilon_1^2}. \tag{48}$$

The complete solution over the interval $[t_i, t_{i+1})$ is as before given by equations (39) through (42) with the only exception that α_i is now given by

$$\alpha_i = [4\varepsilon_2 \{\beta(x_i) - 1\} - \varepsilon_1^2]^{1/2}. \tag{49}$$

The rest of the operations along with the corresponding equations, namely equations (43) through (45), remain identical.

5.3. VAN DER POL'S OSCILLATOR

The normalized form of Van der Pol's oscillator is as shown in equation (6). Here, again, a comparison with equations (28) and (32) shows that the following is a valid choice

$$\begin{aligned} c &= -2\pi\varepsilon_1, \\ k &= 4\pi^2\varepsilon_2, \\ \xi(x, \dot{x}) &= 8\pi\varepsilon_1 x^2\dot{x}. \\ \xi_1(x) &= 8\pi\varepsilon_1 x^2. \end{aligned} \tag{50}$$

The equivalent linear equation (33) now may be written down in the form

$$\ddot{x} + 2\pi\varepsilon_1 \eta_i(x_i)\dot{x} + 4\pi^2\varepsilon_2 x = 4\pi^2\varepsilon_3 \cos(2\pi t). \tag{51}$$

Mean square error minimization leads to

$$\eta_i(x_i) = x_i^2 + x_i \Delta_i + \Delta_i^2/3. \tag{52}$$

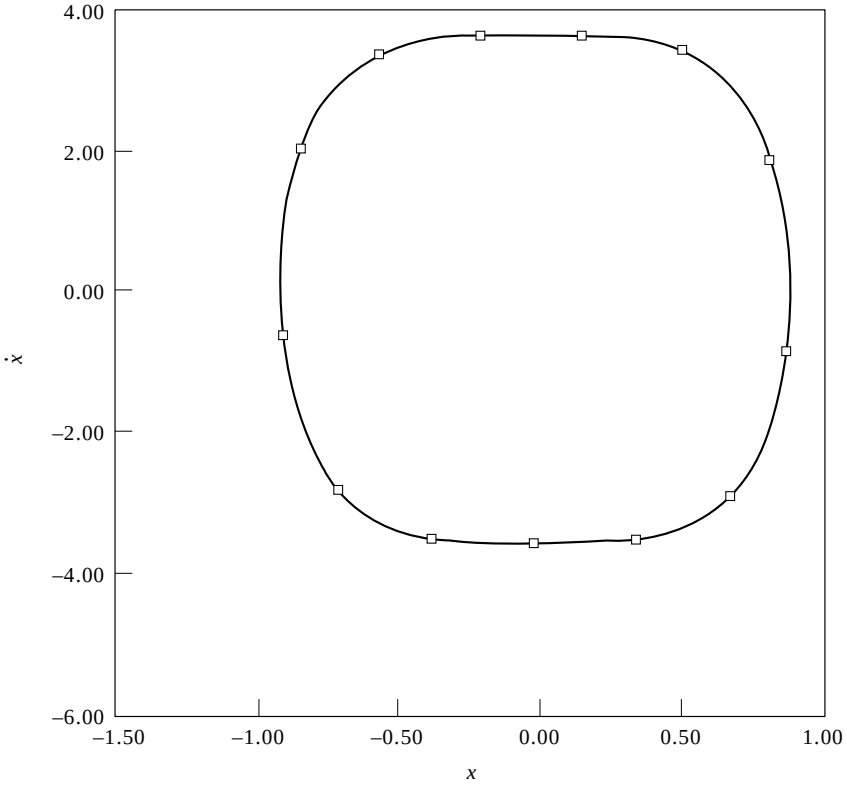

Figure 6. Undamped, unforced phase plane of Ueda's equation: $\varepsilon_1 = 0{\cdot}0$, $\varepsilon_2 = 1{\cdot}0$, $\varepsilon_3 = 0{\cdot}0$, $x_0 = 0{\cdot}9$, $\dot{x}_0 = 0{\cdot}0$. □□□□, Linearization; ——, Runge-Kutta.

The pair of eigenvalues are

$$^{i}\lambda_{1,2} = -\pi\varepsilon_1\,\eta_i\,(x_i) \pm \pi\{\varepsilon_1^2\,\eta_i\,(x_i)^2 - 4\varepsilon_2\}^{1/2}. \tag{53}$$

The particular solution is

$$p_i\,(t) = \frac{1}{D}\,\{\varepsilon_3\,(\varepsilon_2 - 1)\cos(2\pi t) + \varepsilon_1\,\varepsilon_3\,\eta_i\,(x_i)\sin(2\pi t)\}, \tag{54}$$

where

$$D = (\varepsilon_3 - 1)^2 + \varepsilon_1^2\,\eta_i\,(x_i)^2. \tag{55}$$

The complete solution is now given by equation (40). However, if $^{i}\lambda_{1,2}$ are complex conjugates, the functions F_{1i} and F_{2i} take the form

$$\begin{aligned} F_{1i} &= \exp\{-\pi\varepsilon_1\,\eta_i\,(t - t_i)\}\,\{K_{1i}\cos(\pi\alpha_i\,t) + K_{2i}\sin(\pi\alpha_i\,t)\} + p_i\,(t),\\ F_{2i} &= -\pi\varepsilon_1\,\eta_i\exp\{-\pi\varepsilon_1\,\eta_i\,(t - t_i)\}\,\{K_{1i}\cos(\pi\alpha_i\,t) + K_{2i}\sin(\pi\alpha_i\,t)\},\\ &\quad + \pi\alpha_i\exp\{-\pi\varepsilon_1\,\eta_i\,(t - t_i)\}\,\{K_{1i}\cos(\pi\alpha_i\,t) + K_{2i}\sin(\pi\alpha_i\,t)\},\\ \alpha_i &= \{4\varepsilon_2 - \varepsilon_1^2\,\eta_i\,(x_i)^2\}^{1/2}. \end{aligned} \tag{56}$$

The remaining set of operations are precisely the same as in the previous two cases.

5.4. NUMERICAL RESULTS

It would now be appropriate to obtain some numerical results in order to substantiate the previous analysis. First, the phase plots of the undamped and unforced Ueda's and

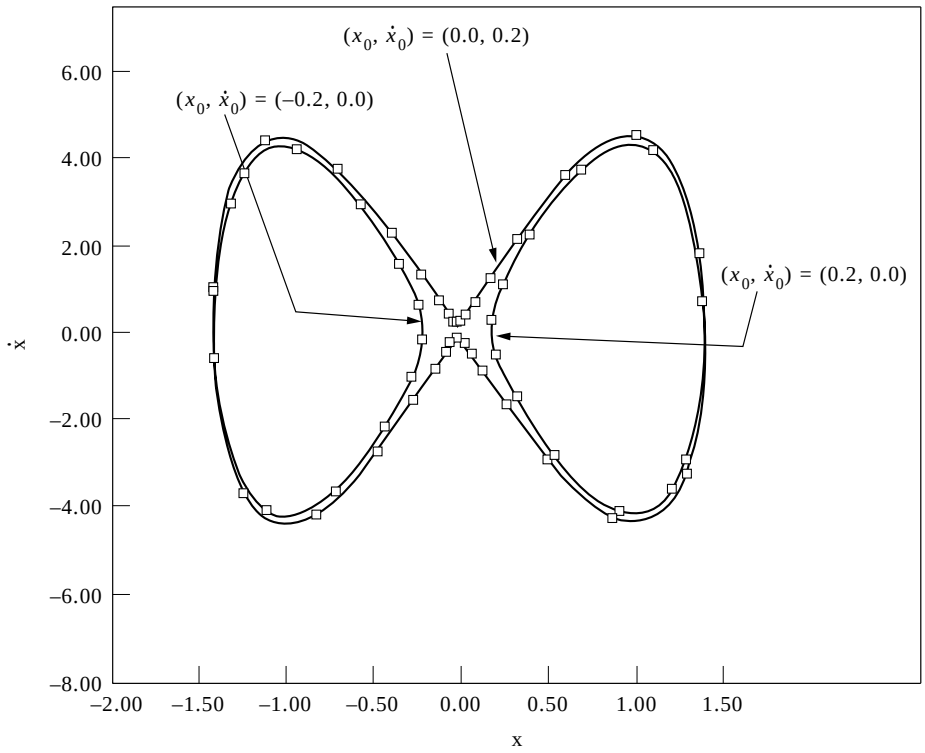

Figure 7. Undamped, unforced phase plane of Duffing-Holmes' equation: $\varepsilon_1 = 0{\cdot}0$, $\varepsilon_2 = 1{\cdot}0$, $\varepsilon_3 = 0{\cdot}0$. ——, Linearization; □□□□, Runge-Kutta.

Duffing–Holmes' oscillators via the present method and a fourth order Runge-Kutta routine are shown in Figures 6 and 7. The unforced and damped Van der Pol's oscillator given by equation (6) with $\varepsilon_3 = 0$, possesses a limit cycle and this is shown in Figure 8. The time-steps, h_i, have been uniformly fixed at 0·02 for all the cases. It may be observed that the comparison is extremely good in all these cases. With the inclusion of forcing and damping, all the three oscillators are capable of showing a variety of one-periodic orbits. Some of these orbits are reported in Figure 9–11. Corresponding solutions via the Runge-Kutta routine are also shown in all these figures. The comparison is again found to be extremely favourable.

6. ACCUMULATION OF ERRORS IN THE NEW METHOD

Unlike the Runge-Kutta method, there is at present no viable way to predict the error that gets accumulated in the process of time marching using the new piecewise linearization scheme. However, the level of approximation achieved by the new method may be conveniently checked against the exact solution of a non-linear ODE. With this in view, the first order ODE

$$\dot{x} + x^2 = 0, \tag{57}$$

is solved. Thus, with the initial condition $x_0 = 1$, the complete solution is

$$x(t) = \frac{1}{1+t}. \tag{58}$$

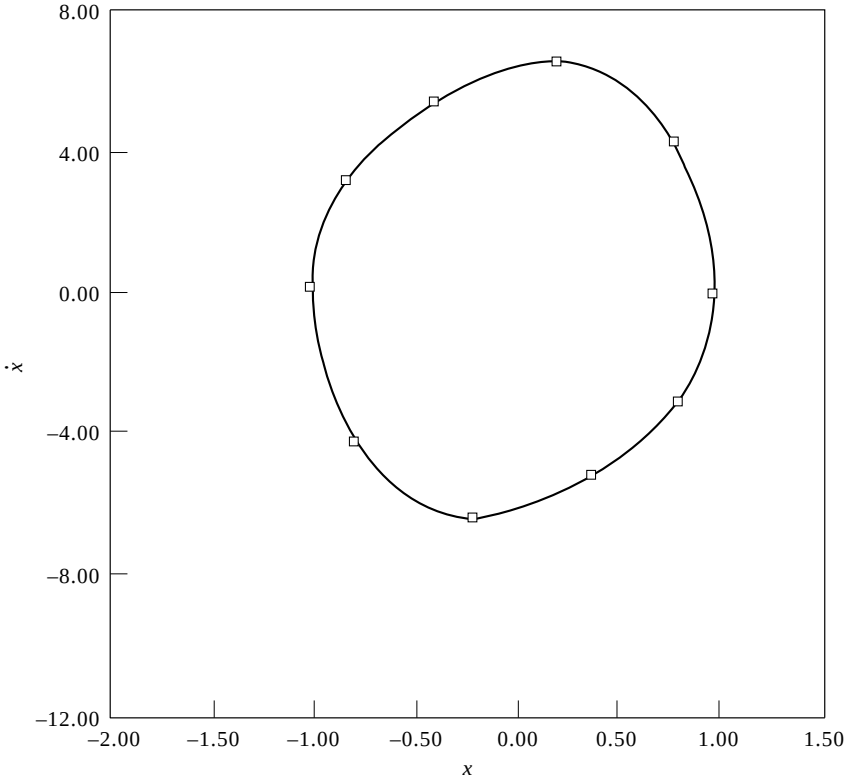

Figure 8. Self-excited limit cycle in unforced Van der Pol's oscillator: $\varepsilon_1 = 0{\cdot}25$, $\varepsilon_2 = 1{\cdot}0$, $\varepsilon_3 = 0{\cdot}0$. □□□□, Runge-Kutta; ——, Linearization.

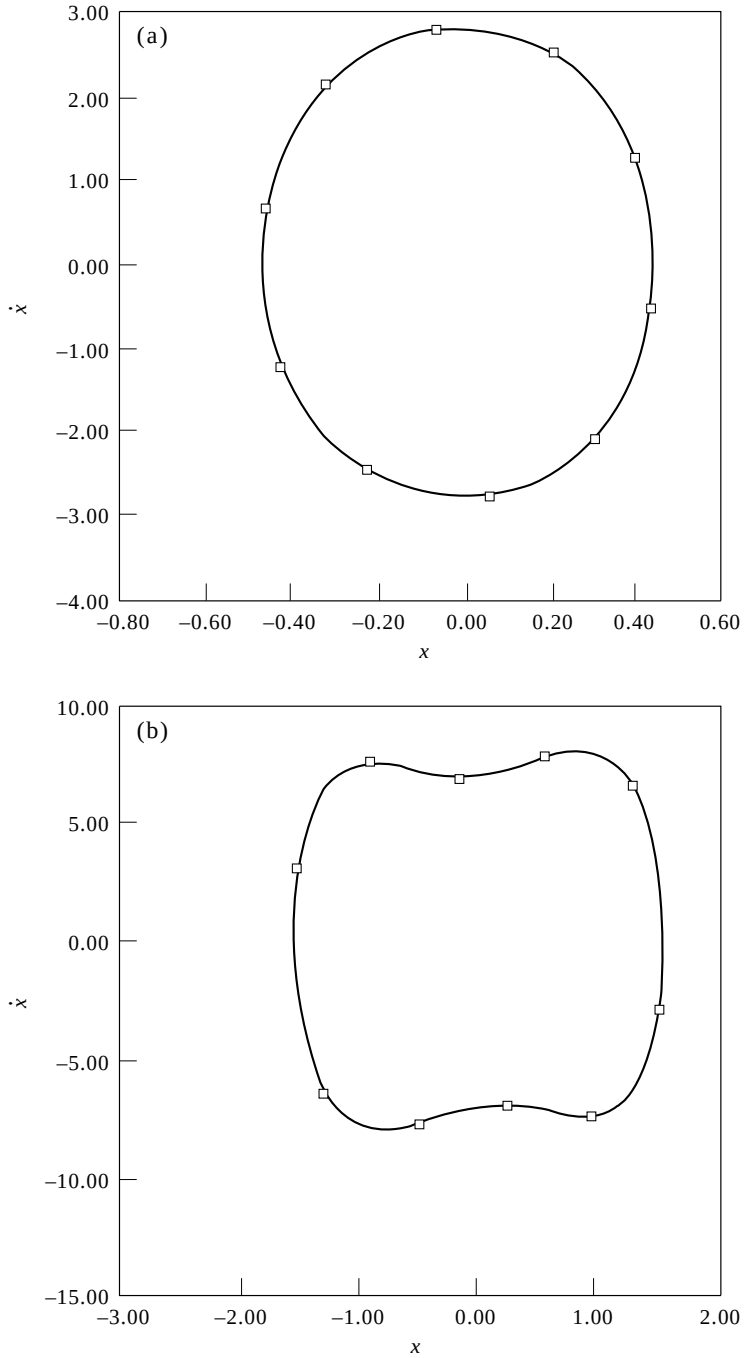

Figure 9. Two kinds of one-periodic orbits for Van der Pol's oscillator: (a) $\varepsilon_1 = 0{\cdot}25$, $\varepsilon_2 = 1{\cdot}0$, $\varepsilon_3 = 0{\cdot}4$; (b) $\varepsilon_1 = 0{\cdot}25$, $\varepsilon_2 = 1{\cdot}0$, $\varepsilon_3 = 1{\cdot}0$. ——, Runge-Kutta; □□□□, Linearization.

Now, to make use of the new linearization scheme for solving equation (57), it is necessary to write it in the equivalent linear form

$$\dot{x} + \beta(x_i, \Delta_i)x = 0, \tag{59}$$

valid over the interval $[t_i, t_{i+1})$. Following an error minimization over $[x_i, x_{i+1})$, the expression for β may be derived as

$$\beta(x_i, \Delta_i) = \frac{3\Delta_i^3 + 12x_i\Delta_i^2 + 18x_i^2\Delta_i + 12x_i^3}{4\Delta_i^2 + 12x_i\Delta_i + 12x_i^2}. \tag{60}$$

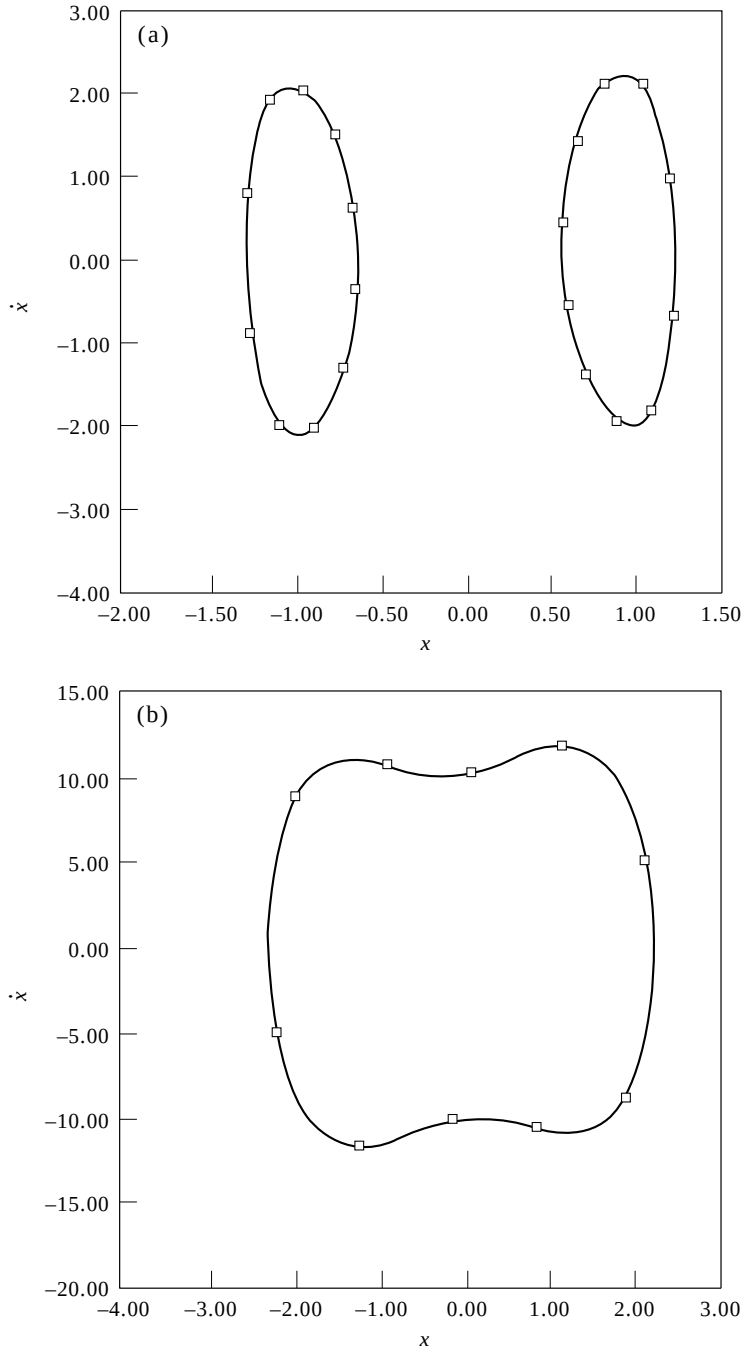

Figure 10. Two kinds of one-periodic orbits for Duffing-Holmes' oscillator: (a) $\varepsilon_1 = 0{\cdot}25$, $\varepsilon_2 = 0{\cdot}5$, $\varepsilon_3 = 0{\cdot}1$; (b) $\varepsilon_1 = 0{\cdot}25$, $\varepsilon_2 = 0{\cdot}5$, $\varepsilon_3 = 0{\cdot}8$. ——, Linearization; □□□□, Runge-Kutta.

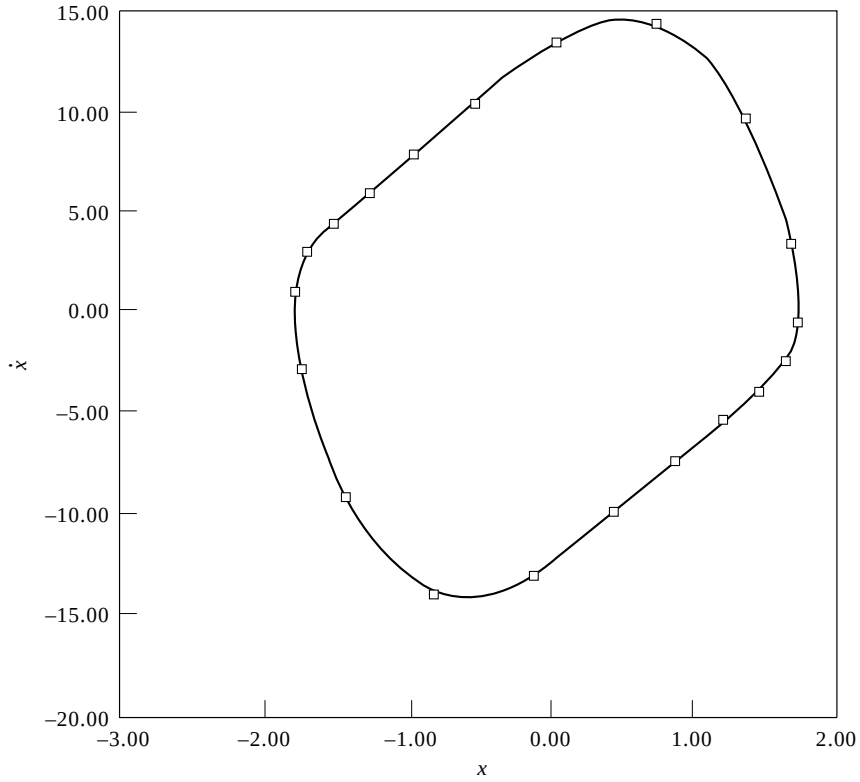

Figure 11. One-periodic orbits for Van der Pol's oscillator: (a) $\varepsilon_1 = 0{\cdot}25$, $\varepsilon_2 = 1{\cdot}0$, $\varepsilon_3 = 1{\cdot}0$; ——, Linearization; □□□□, Runge-Kutta.

The local linearized solution is

$$x(t) = K(x_i) \exp\{-\beta(x_i, \Delta_i)\,(t - t_i)\}, \qquad t \in [t_i, t_{i+1}), \tag{61}$$

and

$$K(x_0) = 1. \tag{62}$$

Thus, it is clear that the present method approximates the function of equation (58) by a set of exponential functions, each valid over a small segment of the trajectory. In Figure 12, the solution obtained via the piecewise linearization is compared with the exact solution. In the same figure, the errors in the solution trajectories obtained via the present method and the fourth order Runge-Kutta method with respect to the exact solution curve (equation 58) are plotted as a function of time. The time step for integration has been consistently fixed at 0·01. It may be readily observed that the new linearization method results in errors which are considerably less than the Runge-Kutta method.

Now, the case of undamped and unforced Duffing-Holmes's oscillator may be considered. The equations for the homoclinic orbit passing through the saddle point at the origin are

$$x(t) = \pm\sqrt{2}\,\mathrm{sech}\,(2\pi\sqrt{\varepsilon_2}t),$$

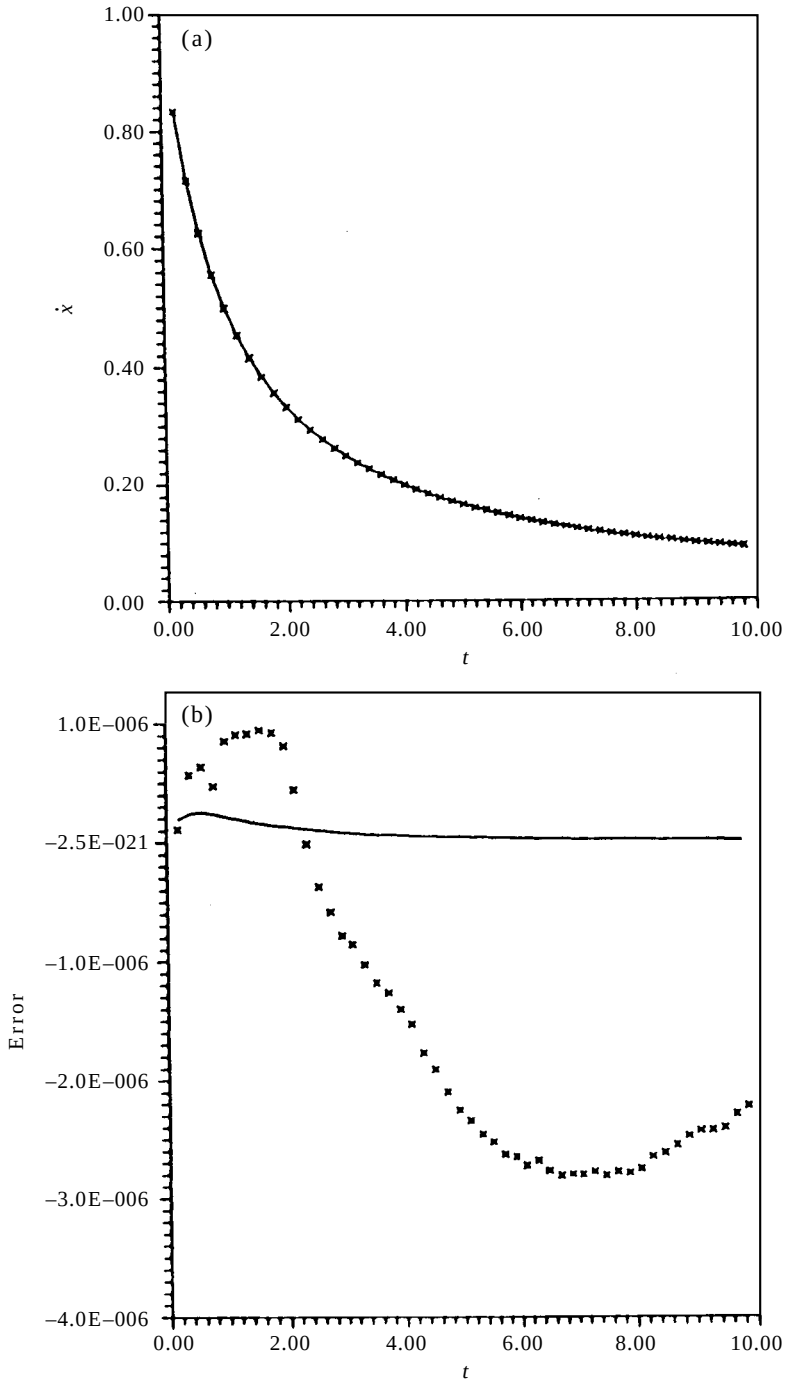

Figure 12. Solutions for an exactly integrable first order ODE: (a) comparison of the linearized solution against the exact solution: ——, Linearization; × × × ×, exact. (b) comparison of errors in Runge-Kutta and linearization: ——, Linearization; × × × ×, Runge-Kutta.

$$\dot{x}(t) = \pm 2\pi\sqrt{2\varepsilon_2}\,\mathrm{sech}\,(2\pi\sqrt{\varepsilon_2}t)\,\tanh\,(2\pi\sqrt{\varepsilon_2}t). \tag{63}$$

Other than the saddle, the homoclinic orbit intersects the x-axis at $\{-\sqrt{2}, 0\}$ and $\{\sqrt{2}, 0\}$. This orbit being an invariant curve, if one starts at anyone of these intersection points, one should reach the saddle asymptotically as the ODE is integrated forward or backward in time. However, in practice, numerical errors creep in and this would result in the solution deviating from the actual homoclinic orbit and ending up on a periodic trajectory. Hence, the robustness of a numerical scheme can be evaluated by finding how closely the solution approaches the saddle. In order to have this type of comparison between the Runge-Kutta and the proposed linearization schemes, the results of numerical integrations of a trajectory starting from $\{\sqrt{2}, 0\}$ using both the methods is shown in Figure 13. Moreover, the errors that accrue in time marching, using the Runge-Kutta and the linearization methods, are tabulated in Table 1. The errors are computed with respect to the exact solution given by equation (63). Here again, it is found that the orbit integrated via the new linearization method approaches the saddle more closely, thereby indicating a lower accumulation of errors.

7. APPLICATIONS OF THE PSL

The phase space linearization method presented in the previous section effectively reduces a non-linear ODE to a non-linear map like all other numerical integration methods. However, unlike other methods, here the form of the map is quite explicit. Moreover, the local flow structure is also uniquely determined explicitly in terms of the dependent variables $\{x_i, \dot{x}_i\}$ and time. Each local solution consists of a free vibration part and a forced vibration part. In case the system is unforced, the eigenvalues of the complementary part alone would furnish complete information about the local structure of the flow. This aspect can be conveniently used for getting several useful information about the oscillator, which may not be the case with other numerical integration schemes.

7.1. DAMPED SEPARATRICES

First, the case of damped, but unforced Duffing-Holmes' oscillator is considered. The damped separatrix of the Duffing-Holmes' oscillator may be readily recognized as the damped stable manifold passing through the saddle at $\{0, 0\}$. As $t \to \infty$, any point on this invariant manifold approaches the saddle. It may also be recalled that via phase space linearization it is possible to reduce Duffing-Holmes' oscillator to a map given by

$$\begin{aligned} x_{i+1} &= F_{1i}\,(x_i, \dot{x}_i, {}^i\lambda_{1,2}, \Delta_i, t_{i+1}, h_i), \\ x_{i+2} &= F_{2i}\,(x_i, \dot{x}_i, {}^i\lambda_{1,2}, \Delta_i, t_{i+1}, h_i). \end{aligned} \tag{64}$$

Sufficiently near the saddle, the eigenvalues ${}^i\lambda_{1,2}$ of the complementary function of the linearized equation over the interval $[t_i, t_{i+1})$ are both real, one being positive and the other negative. Further, for the present case, the stable manifold locally belongs to a one-dimensional eigenspace spanned by the eigenvector corresponding to the negative eigenvalue, say, ${}^i\lambda_2$. Similarly, the unstable manifold is locally spanned by the eigenvector corresponding to the positive eigenvalue, ${}^i\lambda_1$. The unstable manifold goes asymptotically to either of the stable sinks at $\{\pm 1, 0\}$.

Now, to obtain the damped separatrix, it is necessary to start off at the saddle, since it is the only point on the separatrix known *a priori*. The solution curve for any trajectory near the saddle would be

$$x(t) = K_{1i}\exp({}^i\lambda_1\, t) + K_{2i}\exp({}^i\lambda_2\, t), \tag{65}$$

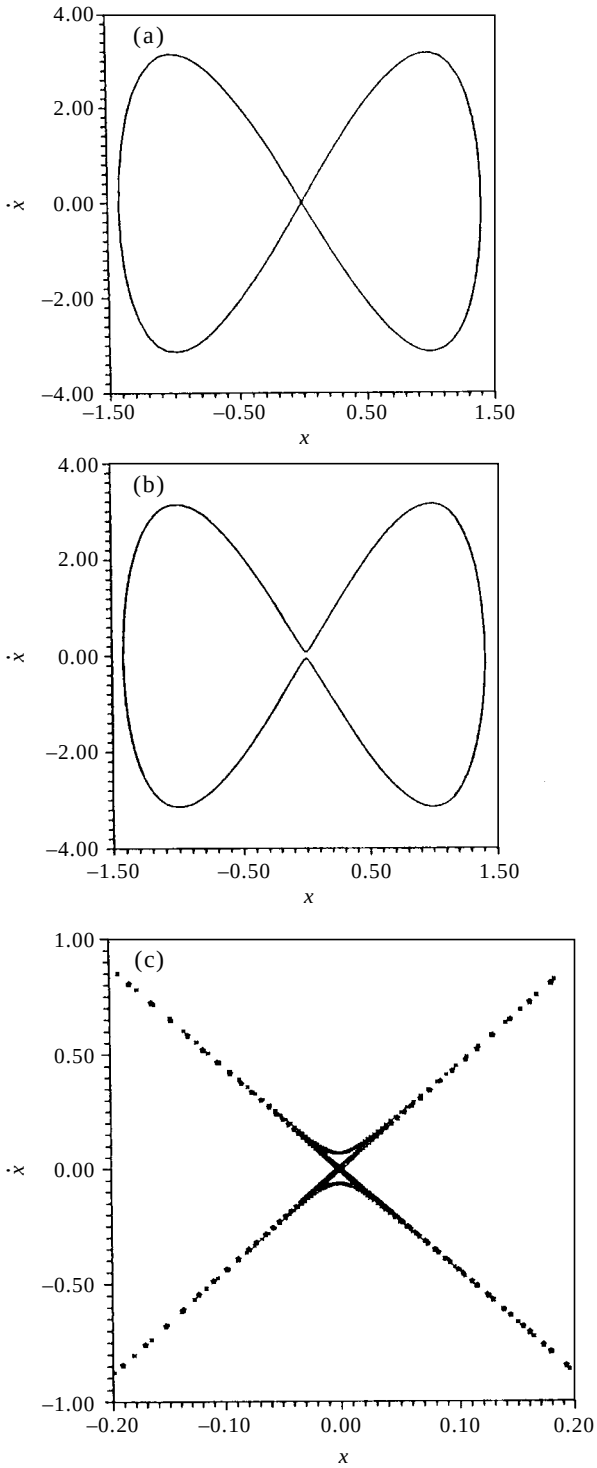

Figure 13. Comparison of errors accumulated for an initial condition on the homoclinic orbit $x(0) = 1{\cdot}4142136$, $\dot{x}_0 = 0{\cdot}0$: (a) PSL; (b) Runge-Kutta. (c) Blow-up of the numerically integrated trajectories near the saddle point: ■ ■ ■ ■, Runge-Kutta; ****, linearization.

TABLE 1

Comparison of errors in RKGS and PSL

x	$\dot{x}$ RKGS	$\dot{x}$ PSL	$\dot{x}$ Exact	Error in RKGS	Error in PSL
1·200	−2·815150	−2·815252	−2·821143	−0·005993	−0·005891
1·100	−3·070021	−3·071108	−3·071539	−0·001518	−0·000431
1·000	−3·141523	−3·141592	−3·141593	−0·000070	−0·000001
0·900	−3·085703	−3·085751	−3·084366	0·001337	−0·001385
0·800	−2·934274	−2·931302	−2·930956	0·003318	−0·000346
0·700	−2·702619	−2·702616	−2·702318	0·000301	−0·000298
0·600	−2·414754	−2·415733	−2·413921	0·000833	−0·001812
0·500	−2·075357	−2·076341	−2·077968	−0·002611	−0·001627
0·450	−1·901321	−1·897123	−1·895382	0·005939	0·001741
0·400	−1·702092	−1·703038	−1·704586	−0·002494	−0·001548
0·350	−1·511451	−1·508321	−1·506634	0·004817	0·001687
0·300	−1·304932	−1·304785	−1·302530	0·002402	0·002255
0·250	−1·094521	−1·091446	−1·093228	0·001293	−0·001782
0·200	−0·880228	−0·880012	−0·879646	0·000582	0·000366
0·150	−0·663855	−0·661918	−0·662673	0·001182	−0·000755
0·100	−0·443245	−0·443238	−0·443176	0·000069	0·000062
0·050	−0·222310	−0·222018	−0·222005	0·000305	0·000013
0·025	−0·111329	−0·110372	−0·110547	0·000782	−0·000175
0·010	−0·053723	−0·0479060	−0·044277	0·009446	−0·003629
0·001	−0·008416	−0·003950	−0·004428	0·003988	−0·000478
0·000	−0·007260	0·002016	0·000000	0·007260	−0·002016

$$x(t) = K_{1i} \exp({}^{i}\lambda_1 t) + K_{2i} \exp({}^{i}\lambda_2 t), \tag{65}$$

where

$$\begin{aligned} {}^{i}\lambda_1 &= -0{\cdot}5\delta_1 + 0{\cdot}5\{\delta_1^2 - 4\delta_2(\beta - 1)\}^{1/2} > 0, \\ {}^{i}\lambda_2 &= -0{\cdot}5\delta_1 - 0{\cdot}5\{\delta_1^2 - 4\delta_2(\beta - 1)\}^{1/2} < 0. \end{aligned} \tag{66}$$

Here, the coefficient β is given by

$$\beta(x_i, \Delta) = \frac{(x_i^4 + 2x_i^3 \Delta_i + 2x_i^2 \Delta_i^2 + x_i \Delta_i^3 + \Delta_i^4/5)}{(x_i^2 + x_i \Delta_i + \Delta_i^2/3)}. \tag{67}$$

On the separatrix, $K_{1i} = 0$. This is because of the fact that $x(t) \to 0$ as $t \to \infty$. Thus, an explicit relationship between x and $\dot{x}$ can be obtained for all points on the separatrix near the saddle. This will be

$$\dot{x}_{i+1} = {}^{i}\lambda_2(x_i, \delta_i) x_{i+1}. \tag{68}$$

Further,

$$t_{i+1} = \{1/{}^{i}\lambda_2(x_i, \Delta_i)\} \ln(x_{i+1}), \tag{69}$$

in deriving equation (69), it has been arbitrarily assumed that $K_{2i} = 1{\cdot}0$. Any other finite value of K_{2i} would simply mean a finite translation along the time axis. However, this

arbitrariness would only affect the parameterization by time, which is inconsequential in so far as the interest is focused on obtaining a correct phase plane plot of x versus $\dot{x}$. An important inference that can be drawn from equation (68) is that the Jacobian of transformation given by

$$|J| = \det \begin{bmatrix} \partial x_{i+1}/\partial x_i & \partial x_{i+1}/\partial \dot{x}_i \\ \partial \dot{x}_{i+1}/\partial x_i & \partial \dot{x}_{i+1}/\partial \dot{x}_i \end{bmatrix}, \tag{70}$$

is identically zero on the damped separatrix. It is interesting to note that the separatrix and the unstable manifold are the only two invariant manifolds on which $|J| = 0$ identically in the damped phase plane.

As one moves away from the saddle, from a point onwards at around $x_1 = 1{\cdot}0$ for some i, equations (68) and (69) are no longer valid, since the eigenvalues ${}^i\lambda_{1,2}$ become complex. Therefore it is reasonable to proceed with equations (68) and (69) upto $x_i < 1$, say, $x_i \approx 0{\cdot}8$, and then use the last obtained values of x_i, $\dot{x}_i$ and t_i to proceed further backwards using the new linearization scheme. The only difference here would be that the time-axis is partially ordered such that $t_i > t_{i+1}$ for all i. During this backward marching, build-up of some numerical error is not ruled out. However, such errors may be conveniently tackled using the fact that $|J| = 0$, as follows. Let, for example, ${}^i\lambda_{1,2}$ both be real. A point on the damped separatrix at $t = t_{i+1}$ would then be given by

$$\begin{aligned} x_{i+1} &= K_{1i} \exp({}^i\lambda_1 t_{i+1}) + K_{2i} \exp({}^i\lambda_2 t_{i+1}), \\ \dot{x}_{i+1} &= {}^i\lambda_1 K_{1i} \exp({}^i\lambda_1 t_{i+1}) + {}^i\lambda_2 K_{2i} \exp({}^i\lambda_2 t_{i+1}) + R_{i+1}(x_i, \dot{x}_i). \end{aligned} \tag{71}$$

Here R_{i+1} is a function designed to nullify the numerical error at $t = t_{i+1}$. R_{i+1} is now chosen in the form

$$R_{i+1} = E_{i+1}(x_i^2 + \dot{x}_i^2)^{1/2}. \tag{72}$$

An equation to determine E_{i+1} may be found from

$$J(E_{i+1}) = 0. \tag{73}$$

It may be pointed out here that the analysis of the damped separatrices as presented in the above two sections applies to many other damped non-linear oscillators, where such separatrices exist. This is true even for a class of oscillators where the vector field is not always C^r, $r \geq 1$. As an example, the piecewise linear viscously damped backlash oscillator, as described earlier, may again be considered. The equations of motion are reproduced below.

$$\begin{aligned} &\ddot{x} + \varepsilon_1 \dot{x} = 0, \qquad |x| < h, \\ &\ddot{x} + \varepsilon_1 \dot{x} + \varepsilon_2 (x - h \operatorname{sgn} x) = 0, \qquad |x| \geq h. \end{aligned} \tag{74}$$

Here h is a positive real number. Previously, a power series approach was formulated to obtain the separatrix, separating the basins of attraction of uncountable infinity for the neutrally stable sinks lying either side of the origin. In order to find out this separatrix, the linearization approach is more convenient to adopt since the original equation itself is piecewise linear. Thus the separatrix of equation (74) near the point, $\{x_0, y_0\} = \{0, 0\}$, is written as

$$\begin{aligned} x &= K_{20} \exp(-\varepsilon_1 t), \\ \dot{x} &= \varepsilon_1 K_{20} \exp(-\varepsilon_1 t). \end{aligned} \tag{75}$$

A comparison of x and $\dot{x}$ in the above equation leads to

$$\dot{x} = -\varepsilon_1 x. \tag{76}$$

The above relationship is valid so long as $|x| < h$. To proceed beyond $|x| = h$, it is necessary to find the time, t, at which $|x| = h$. As an illustration, let t_h^1 be the time at which $x = h$. Now, arbitrarily assigning $K_{20} = 0$, as per the arguments presented earlier in this section, it can be readily shown that

$$t_h^1 = -(1/\varepsilon_1) \ln h. \tag{77}$$

No equation (74) may be solved for $x > h$, with the initial conditions

$$\begin{aligned} x_1 &= h, \\ \dot{x}_1 &= -\varepsilon_1 h, \\ t_1 &= t_h^1. \end{aligned} \tag{78}$$

Thus, for example, for $\varepsilon_1^2 < 4\varepsilon_2$, the solution is given by

$$\begin{aligned} x(t) &= \exp(-0{\cdot}5\varepsilon_1 t)\,(K_{11} \cos(\alpha t) + K_{21} \sin(\alpha t)), \\ \dot{x}(t) &= -0{\cdot}5\varepsilon_1 (x - h) + \exp(-0{\cdot}5\varepsilon_1 t)\,(K_{21}\,\alpha \cos(\alpha t) - K_{11}\,\alpha \sin(\alpha t)), \\ \alpha &= 0{\cdot}5\sqrt{4\varepsilon_2 - \varepsilon_1^2}, \\ K_{11} &= -(1/\alpha)\dot{x}_1 \exp(0{\cdot}5\varepsilon_1 t_1) \sin(\alpha t_1), \\ K_{21} &= (1/\alpha)\dot{x}_1 \exp(0{\cdot}5\varepsilon_1 t_1) \cos(\alpha t_1). \end{aligned} \tag{79}$$

Similar solutions can be constructed for $\varepsilon_1^2 > 4\varepsilon_2$. Moreover, using this algorithm, backward marching in time may be made away from the saddle and the damped separatrix can be obtained.

7.2. UNSTABLE LIMIT CYCLES

For the harmonically forced Duffing-Holmes oscillator with sufficiently small forcing amplitude parameter, ε_3, a one-periodic symmetric limit cycle exists surrounding the origin. Here the interest would be in finding this orbit using the phase space linearization scheme. It may be noted that, the separatrix of the basins of attraction of the pair of stable one-periodic orbits starts from different points on the unstable limit cycle depending on the initial time instant $t_0 = \phi$. Such a variation of the perturbed separatrix is however periodic in ϕ with the same period as that of the external forcing. With this in view, it would be convenient to translate the time axis as

$$\bar{t} = t + \phi. \tag{80}$$

Effecting this translation in equation (3), one gets

$$\ddot{x} + 2\pi\varepsilon_1 \dot{x} + 4\pi^2\varepsilon_2 (x^3 - x) = 4\pi^2\varepsilon_3 \cos(2\pi\bar{t} + \phi), \tag{81}$$

where ϕ is modulo 1. In what follows, $\bar{t}$ will be uniformly replaced by t for notational convenience.

Though structurally unstable, the limit cycle around the origin is an invariant manifold of the non-linear flow. Thus, under forward and backward iterates of the vector function $\mathbf{F}_i = \{F_{1i}\ F_{2i}\}$ given by equation (45), any given point would remain on the orbit. Let any point $\{{}^u x_i, {}^u \dot{x}_i\}$ on the unstable limit cycle be chosen. It is now useful to investigate the stable and unstable eigenspaces of the linearized flow at $\{{}^u x_i, {}^u \dot{x}_i\}$, making use of the PSL scheme. Considering a closed-open segment $I = [\{{}^u x_i, {}^u \dot{x}_i\},\ \{{}^u x_{i+1}, {}^u \dot{x}_{i+1}\})$ and any point

${}^{u}\mathbf{x} = \{{}^{u}x, {}^{u}\dot{x}\} \in I$, the method of PSL permits one to construct a linear ODE for $\mathbf{x}$ which closely approximates the non-linear ODE over I. The two eigenvalues required to construct the complementary function of this linear ODE are given by

$$
\begin{aligned}
{}^{i}\lambda_1 &= -\pi\varepsilon_1 + \pi\{\varepsilon_1^2 + 4\varepsilon_2(1-\beta)\}^{1/2},\\
{}^{i}\lambda_2 &= -\pi\varepsilon_1 - \pi\{\varepsilon_1^2 + 4\varepsilon_2(1-\beta)\}^{1/2},
\end{aligned}
\tag{82}
$$

where, $\beta = \beta({}^{u}x_i, \Delta_i)$ is given by equation (36). If attention is restricted to the point $\{{}^{u}x_i, {}^{u}\dot{x}_i\}$ then it follows

$$
\beta({}^{u}x_i, \Delta_i) = \beta({}^{u}x_i, 0) = {}^{u}x_i^2. \tag{83}
$$

For the unstable limit cycle, obviously ${}^{u}x_i^2 < 1$. Using this bit of information in equation (71), it is readily seen that the eigenvalues ${}^{i}\lambda_{1,2}$ are always real and that

$$
{}^{i}\lambda_1 > 0 \qquad \text{and} \qquad {}^{i}\lambda_2 < 0. \tag{84}
$$

Let ${}^{i}e_1$ and ${}^{i}e_2$ denote, respectively, the eigenvectors corresponding to ${}^{i}\lambda_1$ and ${}^{i}\lambda_2$. Then the unstable and stable eigenspaces, denoted respectively by ${}^{i}E_u$ and ${}^{i}E_s$, are given by

$$
\begin{aligned}
{}^{i}E_u &= \text{span}\,\{{}^{i}e_1\},\\
{}^{i}E_s &= \text{span}\,\{{}^{i}e_2\},
\end{aligned}
\tag{85}
$$

Since ${}^{i}\lambda_1$ is strictly positive for all i, it is concluded that ${}^{i}E_u$ exists everywhere on the limit cycle. This ensues a structural instability of the limit cycle even under the smallest perturbation. Further, strictly on the limit cycle, it is the stable eigenspace ${}^{i}E_s$ that governs the flow. Thus, the complete solution of the limit cycle over the interval I may be written as

$$
{}^{u}x(t) = K_{2i}\exp({}^{i}\lambda_2\, t) + (1/D)\varepsilon_3\{\varepsilon_2(\beta-1)-1\}\cos 2\pi(t+\phi) + (1/D)\varepsilon_1\,\varepsilon_3 \sin 2\pi(t+\phi), \tag{86}
$$

where

$$
D = \{\varepsilon_2(\beta^2-1)-1\}^2 + \varepsilon_1^2. \tag{87}
$$

Since ${}^{i}\lambda_2$ is strictly negative, the first term on the RHS of equation (86) vanishes as $t \to \infty$. However, a difficulty that still stands in the way of finding this orbit is that not a single point on it is yet known. To overcome this difficulty, a novel argument is presented. Let a Poincaré section based on $\phi = \phi_i$ be chosen. On this section the unstable limit cycle reduces to an unstable perturbed saddle $\{{}^{u}x_i, {}^{u}\dot{x}_i\}$. Moreover, it is noted that t has to start from zero at the saddle as the arbitrariness in choosing the section is reflected in the variable ϕ. Therefore at this perturbed saddle, equation (86) takes the form

$$
{}^{u}x(t) = (1/D)\varepsilon_3\{\varepsilon_2(\beta-1)-1\}\cos(2\pi\phi_i) + (1/D)\varepsilon_1\,\varepsilon_3\sin(2\pi\phi_i). \tag{88}
$$

The above is a transcendental equation in ${}^{u}x_i$. This can be solved for various $\phi_i \in [0, 1)$. Thus the unstable limit cycle is now given by the set of points $\{{}^{u}x_i, {}^{u}\dot{x}_i \,|\, \phi_i \in [0, 1)\}$.

7.3. A CLASS OF STABLE LIMIT CYCLES

In this section, attention is restricted towards finding the one-periodic orbits for a class of oscillators where the origin, $\{0, 0\}$, is a stable fixed point when no forcing is applied. It may be mentioned that for the class of oscillators where a stable sink is located at a point other than the origin, as in the Duffing-Holmes' case, a simple transformation would suffice to convert these systems to the ones satisfying the above requirements. However,

for expedience, Ueda's oscillator as in equation (4) is considered as an illustration. It is known that for a sufficiently small excitation amplitude parameter, ε_3, the oscillator possesses one-periodic limit cycles having a two-sided symmetry about the x and $\dot{x}$ axes. Now, let any point $\{{}^s x_i, {}^s \dot{x}_i\}$ be chosen on this orbit. As in the case of unstable limit cycles, here also the stable and unstable eigenspaces of the complementary part of the linearized flow at $\{{}^s x_i, {}^s \dot{x}_i\}$ needs to be investigated. Considering a closed-open segment $I = [\{{}^s x_i, {}^s \dot{x}_i\}, \{{}^s x_{i+1}, {}^s \dot{x}_{i+1}\})$ and any point ${}^s\mathbf{x} = \{{}^s x, {}^s \dot{x}\} \in I$, the two eigenvalues required to construct the complementary function of the equivalent linear ODE are given by

$$ {}^i\lambda_{1,2} = -\pi\varepsilon_1 \pm \pi\{\varepsilon_1^2 + 4\varepsilon_2 (1 - \beta)\}^{1/2}, \tag{89} $$

where, β is given by equation (36). Moreover, in the limit $\Delta_i \to 0$, it is readily seen that

$$ \text{Re } ({}^i\lambda_{1,2}) \leqslant 0 \; \forall \; s_{x_i}. \tag{90} $$

Thus, as $t \to \infty$, the complementary part of the local solution given by equation (40) goes to zero. Therefore, in the limit as $\Delta_i \to 0$, the solution of the limit cycle may be expressed as

$$ {}^s x_i = A_1 ({}^s x_i) \cos (2\pi t) + A_2 ({}^s x_i) \sin (2\pi t) \tag{91} $$

and

$$ {}^s \dot{x}_i = -2\pi A_1 ({}^s x_i) \sin (2\pi t) + 2\pi A_2 ({}^s x_i) \cos (2\pi t), \tag{92} $$

where

$$ A_1 = \frac{\varepsilon_3 (\varepsilon_2^s x_i^2 - 1)}{(\varepsilon_2 {}^s x_i^2 - 1)^2 + \varepsilon_1^2}, $$

$$ A_2 = \frac{\varepsilon_1 \varepsilon_3}{(\varepsilon_2 {}^s x_i^2 - 1)^2 + \varepsilon_1^2}. \tag{93} $$

It is noted that equation (91) is a non-linear algebraic equation in ${}^s x_i$ for any given $t \in [0, 1)$. Thus, solution of equation (91) followed by the use of equation (92) leads to the solution for the one-periodic orbit. However, instead of solving for ${}^s x_i$ repeatedly from equation (91), the following simple transformation may be resorted to. Let the solution of the orbit be taken in the form

$$ {}^s x = r \cos 2\pi(t - \phi), $$

$$ {}^s \dot{x} = -2\pi r \sin 2\pi(t - \phi). \tag{94} $$

Effecting the transformation $\psi = t - \phi$, it is readily seen that it suffices to know r for obtaining a phase plane representation of the orbit. Let ${}^s\mathbf{x}_{min} = \{{}^s x_{min}, 0\}$ and ${}^s\mathbf{x}_{max} = \{{}^s x_{max}, 0\}$ be the two points of intersection of the orbit with the x-axis, the former on the negative side and the latter on the positive side. Thus, the following relation holds true because of symmetry requirements

$$ -{}^s x_{min} = r = {}^s x_{max}. \tag{95} $$

Since at these points ${}^s x = 0$, it follows from equations (94) that

$$ t = \frac{1}{2\pi} \tan^{-1} \left(\frac{\varepsilon_1}{\varepsilon_2 r^2 - 1} \right). \tag{96} $$

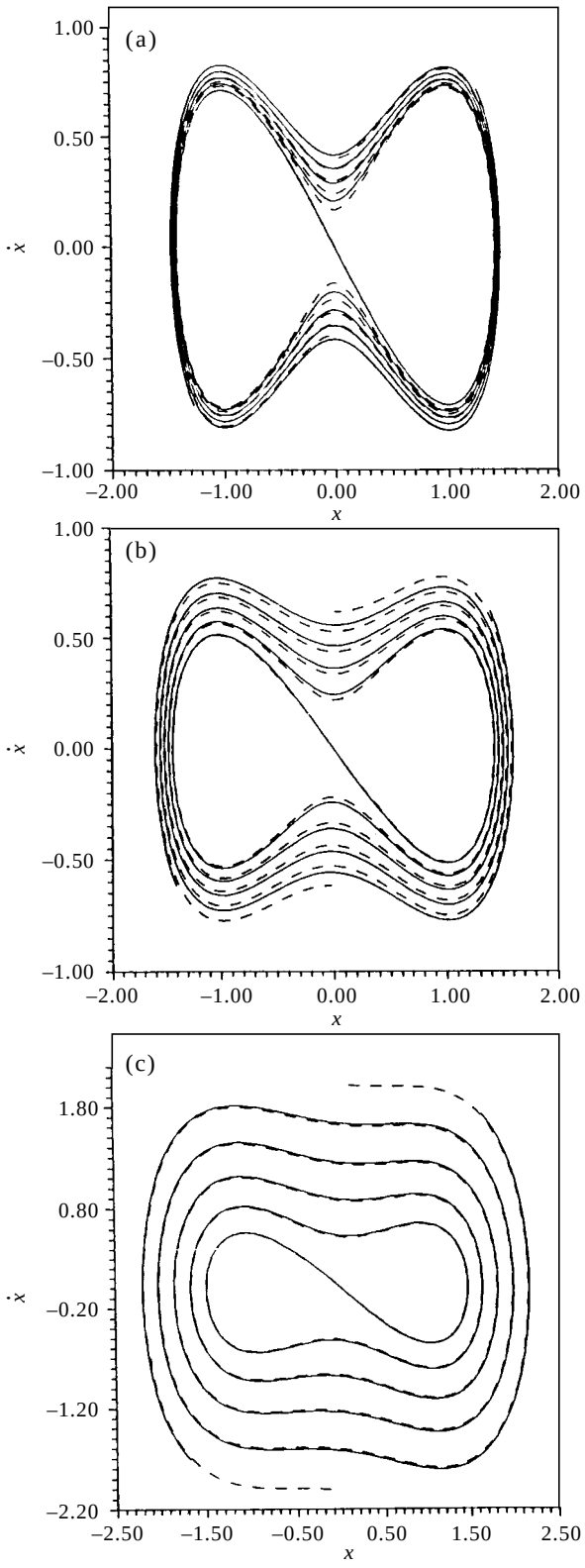

Figure 14. Damped separatrix of Duffing-Holmes' oscillator: (a) $\varepsilon_1 = 0{\cdot}01$, $\varepsilon_2 = 0{\cdot}5$, $\varepsilon_3 = 0{\cdot}0$; (b) $\varepsilon_1 = 0{\cdot}1$, $\varepsilon_2 = 0{\cdot}5$, $\varepsilon_3 = 0{\cdot}0$; (c) $\varepsilon_1 = 0{\cdot}25$, $\varepsilon_2 = 0{\cdot}5$, $\varepsilon_3 = 0{\cdot}0$. ——, Linearization; – – –, power series.

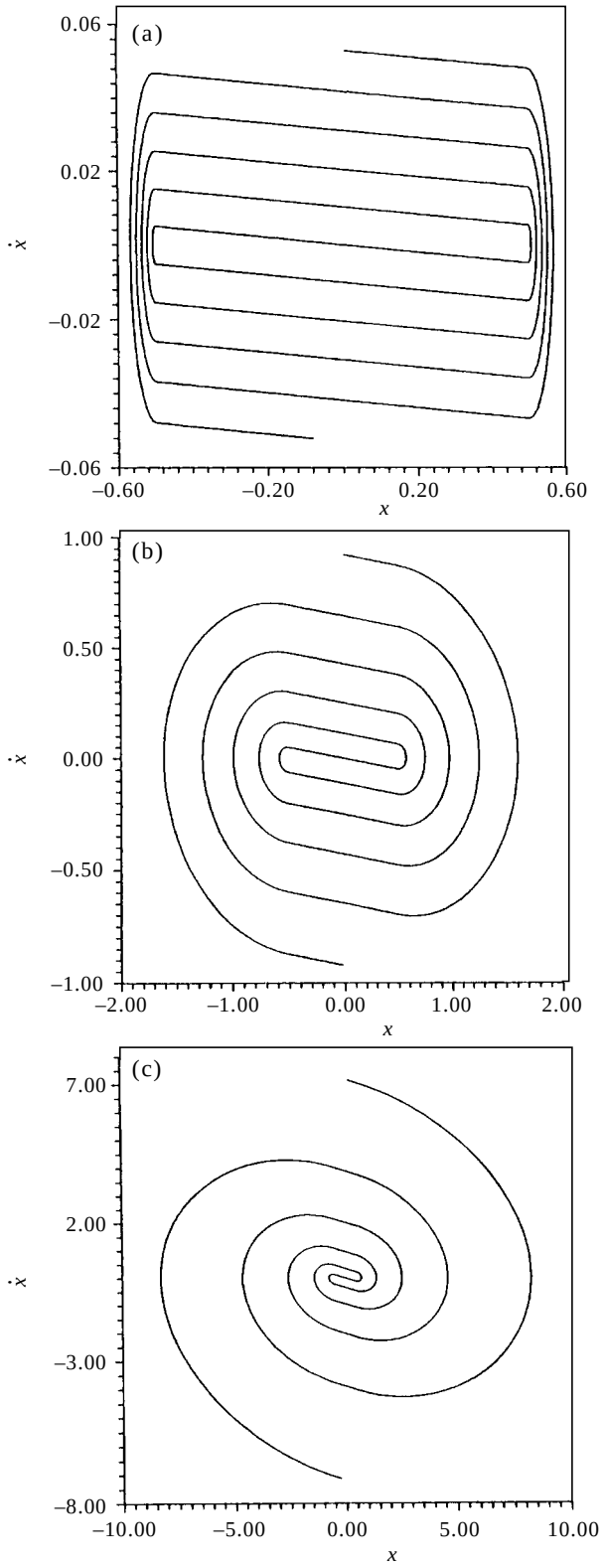

Figure 15. Damped separatrix of the backlash oscillator: (a) $\varepsilon_1 = 0{\cdot}01$, $\varepsilon_2 = 0{\cdot}5$, $h = 0{\cdot}5$; (b) $\varepsilon_1 = 0{\cdot}1$, $\varepsilon_2 = 0{\cdot}5$, $h = 0{\cdot}5$; (c) $\varepsilon_1 = 0{\cdot}25$, $\varepsilon_2 = 0{\cdot}5$, $h = 0{\cdot}5$. ——, Linearization; – – –, power series.

Substitution of the above equation in the first of equations (94) leads to a transcendentalequation in r. Thus, the orbit can be found to a high level of accuracy by solving only a single transcendental equation.

7.4. NUMERICAL RESULTS

To illustrate the above analysis, detailed numerical results have been obtained for all the three oscillators analysed. The damped separatrices of the Duffing-Holmes oscillator as obtained via the linearization procedure are shown in Figure 14 and compared with the ones obtained via the power series approach. The comparison of the two approaches is seen to be extremely favourable except at very low values of damping. For such low values of ε_1, the sharp inward dip of the stable manifold towards the saddle is brought out more accurately by linearization scheme. However, it may be pointed out that the power series approach has been consistently found to be computationally faster. For the backlash oscillator given by equation (74), the damped separatrices have been obtained for three different values of the damping parameter, ε_1, and these are shown in Figure 15. Here the comparison appears to be indistinguishably good. Next, the unstable limit cycle of Duffing-Holmes' oscillator have been obtained for two different values of the excitation parameter, ε_3, and are plotted in Figure 16 along with the stable limit cycles. The

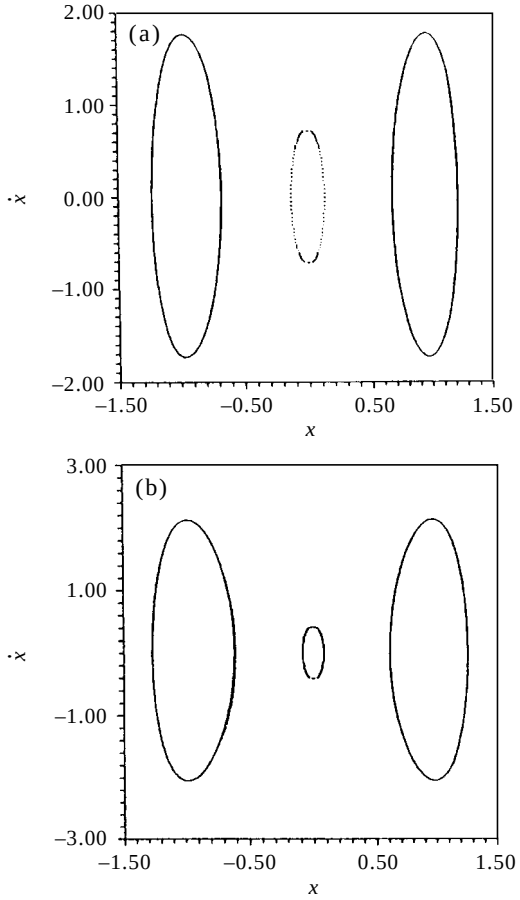

Figure 16. Stable and unstable limit cycles of Duffing-Holmes' oscillator: (a) $\varepsilon_1 = 0{\cdot}25$, $\varepsilon_2 = 0{\cdot}5$, $\varepsilon_3 = 0{\cdot}05$; (b) $\varepsilon_1 = 0{\cdot}25$, $\varepsilon_2 = 0{\cdot}5$, $\varepsilon_3 = 0{\cdot}12$.

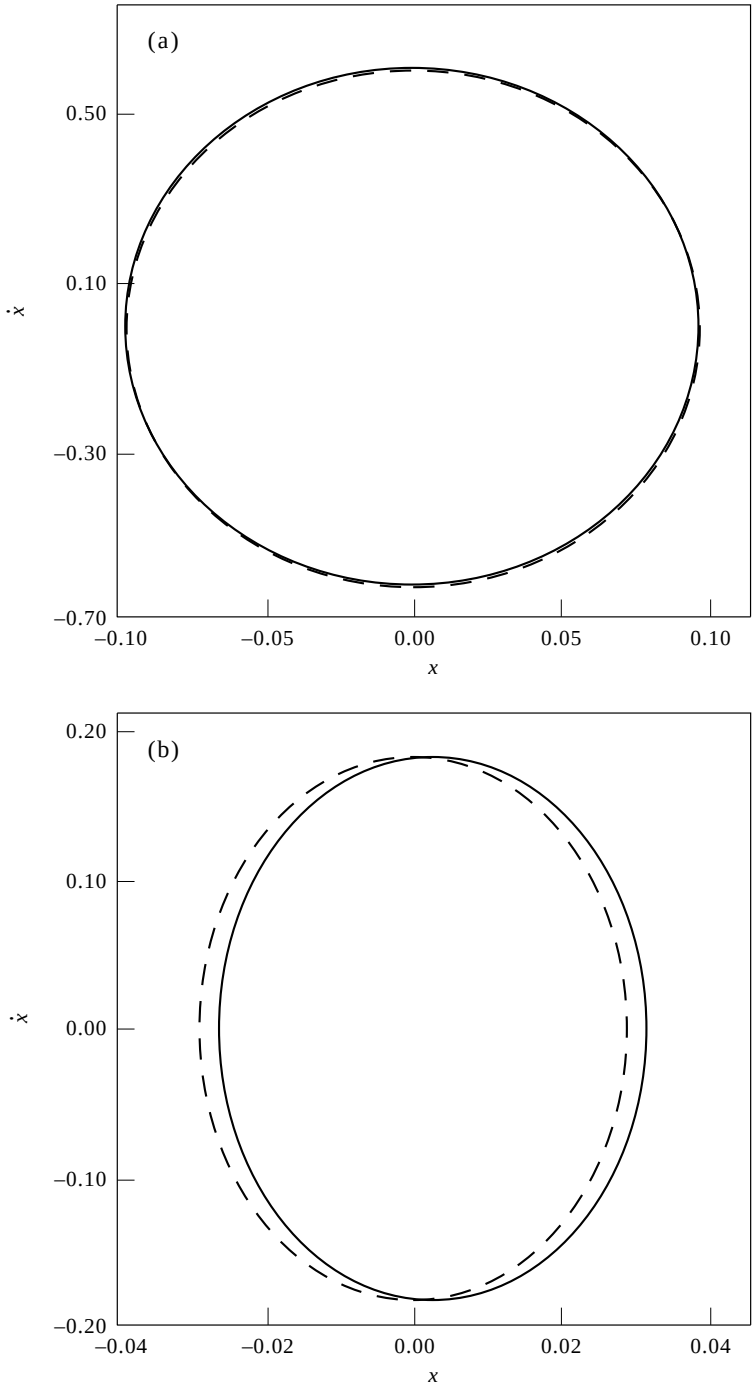

Figure 17. Stable one-periodic orbits of Ueda's oscillator: (a) $\varepsilon_1 = 0{\cdot}25$, $\varepsilon_2 = 1{\cdot}0$, $\varepsilon_3 = 0{\cdot}3$; (b) $\varepsilon_1 = 0{\cdot}25$, $\varepsilon_2 = 1{\cdot}0$, $\varepsilon_3 = 0{\cdot}05$. ——, Simulation; – – –, analytical.

unstable limit cycle is expectedly much smaller in size in comparison with the stable ones. Due to the symmetry of the unstable limit cycles, it suffices to obtain only one half and then generate the other half by reflection. Finally, the stable one-periodic limit cycles of

Ueda's oscillator, as obtained via the technique outlined in section 7.3, are shown in Figure 17 and compared with numerically simulated orbits. The comparisons are found to be favourable.

8. DISCUSSION AND CONCLUSIONS

To begin with, a power series approach is developed to obtain the damped separatrices in second order damped non-linear oscillators. Here, a technique for vaulting the successive poles of the series solution is also discussed in detail. The power series method is functionally similar to the method of continuous analytic continuation, developed earlier by Davis [5]. The method has been found to be very efficient computationally and can easily be programmed in a digital computer. For bringing out the universality of the method, the damped separatrices of two different oscillators, namely Duffing-Holmes' oscillator and the piecewise linear backlash oscillator, have been obtained. An advantage of this analytical approach is that one can quickly find out the asymptotic nature of any trajectory starting from an arbitrary initial condition. Thus, the necessity of an extensive numerical integration is eliminated. This approach is, however, crucially dependent on the fact that at least one point on the separatrix should be known beforehand.

A novel linearization scheme, called phase space linearization, is next developed in this paper for an efficient numerical integration of non-linear ODEs. The idea is to replace the non-linear system in the phase plane by a union of piecewise linear system phase plane trajectories. The non-linear ODE is therefore replaced by a set of linear ODEs whose coefficients become functions of the values of dependent variables at the start of the time intervals over which the linear ODEs are valid. Unlike the usual Runge-Kutta routines, in this new method the increments of the dependent variables over a time interval are calculated using a set of non-linear algebraic equations. However, in the specific case of the non-linear ODE being of the form as given by equation (28), it is required to solve only a transcendental equation. In principle, a transcendental equation may have more than one real root. In the present case, however, the solution trajectory of the ODE is known to be unique depending on the initial conditions. This hints to the fact that it is possible to get a single real root of the transcendental equation for a given time interval h_i. Even though a mathematical proof towards this observation cannot be provided at present, this has been numerically verified to be true without exception. Moreover, to simplify the search for the root, Δ_i, of the transcendental equation (44), it is suggested that an approximate value for Δ_i may be obtained using Taylor's expansion

$$\Delta_i \approx \frac{\mathrm{d}x_i}{\mathrm{d}t} h_i + \frac{\mathrm{d}^2 x_i}{\mathrm{d}t^2} h_i^2 /2! + \frac{\mathrm{d}^3 x_i}{\mathrm{d}t^3} h_i^3 /3! + \ldots . \tag{97}$$

In the above expression, the second and the higher order derivatives of x_i are expressible in terms of x_i and $\mathrm{d}x_i/\mathrm{d}t$ only. The actual root Δ_i should be quite close to the approximate one given by equation (97) and thus the interval of search can be reduced considerably. This observation also helps in making the scheme computationally efficient. Thus, the higher the number of terms in the Taylor expansion (97), less would be the time taken to find out the roots. The procedure has been applied to obtain free vibration and one-periodic forced vibration responses of different kinds of second order non-linear oscillators. From the limited number of results presented, it is seen that the accumulation of errors in the process of time marching is much less in the present method than in the fourth order Runge-Kutta scheme. Moreover, an analysis of the eigenvalue structure of the free vibration part of the locally linearized flow has been found to yield a spectrum of useful information. Thus, it has been shown that it is possible to accurately find out

the damped separatrices of Duffing-Holmes' and backlash oscillators. This also leads to an analytical criterion to obtain a class of stable and unstable limit cycles.

At this stage, it is pertinent to ask whether the technique of phase space linearization can predict the subharmonic, quasi-periodic and chaotic response of non-linear oscillators. Moreover, now that it is possible to have an analytical expression for the unstable limit cycle of Duffing-Holmes' oscillator, it may as well be possible to find out the forced separatrix, separating the basins of attraction of the pair of stable limit cycles. The forced separatrix is essentially the forced stable manifold reaching some point on the unstable limit cycle asymptotically. The forced unstable manifold, on the other hand, originates from the unstable limit cycle. Thus, if both the stable and unstable manifolds can be obtained analytically, it should also be possible to derive information about homoclinic intersections. Thus, it would be interesting to ask whether PSL can be suitably adapted to compute characteristic quantities of the non-linear flow, such as Fourier spectra, Liapunov characteristic exponents and probability density functions. That PSL is indeed versatile in handling these and several other delicate questions demonstrated in the companion paper [9].

REFERENCES

1. S. Margolis, and W. Vogt 1973 *IEEE Transactions on Automatic Control*, **AC — 8**, 104–111. Control engineering application of V. I. Zubov's construction procedure for Liapunov functions.
2. V. I. Zubov 1964 *Methods of Liapunov and their Application*. Groningen: Noordhoff.
3. E. J. Davison and E. M. Kurak 1971 *Automatica* **7**, 627–636. A computational method for determining quadratic Liapunov functions for nonlinear systems.
4. A. Vannelli and M. Vidyasagar 1985 *Automatica* **21**, 69–80. Maximal Liapunov functions and domains of attraction for autonomous nonlinear systems.
5. H. T. Davis 1962 *Introduction to Nonlinear Differential and Integral Equations*. New York: Dover Publications Inc.
6. N. Minorsky 1962 *Nonlinear Oscillations*. Princeton, NJ: Van Nostrand and Co.
7. D. R. J. Chillingworth 1976 *Differential Topology with a View to Applications*. London: Pitman.
8. J. Hale 1980 *Ordinary Differential Equations*. Berlin: Springer-Verlag.
9. R. N. Iyengar and D. Roy 1998 *Journal of Sound and Vibration*, **211,** 877–906. Extensions of the phase space linearization (PSL) technique for non-linear oscillators.